Thesis for the Degree of Doctor of Philosophy

Changes in near-surface winds across Sweden over the past decades

Observations and simulations

Lorenzo Minola

Department of Earth Sciences
Faculty of Science

UNIVERSITY OF GOTHENBURG

Gothenburg, Sweden 2020

Cover illustration: Lorenzo Minola

Photography: Nicoletta Lupi

Changes in near-surface winds across Sweden over the past decades –
Observations and simulations

lorenzo.minola@gmail.com

ISBN 978-91-8009-122-0 (PRINT)
ISBN 978-91-8009-123-7 (PDF)
Available at: http://hdl.handle.net/2077/66844

Printed in Borås, Sweden 2020
Printed by Stema Specialtryck AB

In the memory of my father and grandfather

With his help I discovered that I was not opposed to mankind but only to man-centeredness, anthropocentricity, the opinion that the world exists solely for the sake of man; not to science, which means simply knowledge, but to science misapplied, to the worship of technique and technology, and to that perversion of science proper called scientism; and not to civilization but to culture.

Edward P. Abbey

Summary

Driven by a combination of anthropogenic activities and climate changes, near-surface terrestrial winds displayed a large decrease in their magnitude in the past decades, named "stilling", and a recent recovery in their slowdown. Understanding how wind has changed and identifying the factors behind the observed variabilities is crucial so that reasonable future wind scenarios can be constructed. In this way, adaptation strategies can be developed to increase society's resilience to the plausible future wind climate. This is particularly important for Sweden, which is largely vulnerable to changes in mean wind speed conditions and to the occurrence of extreme winds. Therefore, this thesis investigates past variations in near-surface winds across Sweden and explores the mechanisms behind their variabilities and changes. This is done by using the first homogenized dataset of in-situ observations and by analyzing current simulations of wind gusts.

Results show that, during the past decades, both observed mean and gust wind speed underwent nonlinear changes, driven by the dominant winter variability. In particular, consistent with the stilling-reversal phenomena, the significant stilling ceased in 2003, followed by no clear trend afterwards. The detected stilling-reversal is linked to large-scale atmospheric circulation changes, in particular to the North Atlantic Oscillation, and the intensity changes of extratropical cyclones passing across Sweden. The comparison with reanalysis outputs reveals that, in addition to the large-scale interannual variability, changes in surface roughness (e.g. changes in forest cover) have most likely contributed to the observed wind change across Sweden. Moreover, this thesis finds that current regional climate models and reanalyses do not have adequate skills in simulating past wind gusts across inland and mountain regions. Major improvements are achieved when the elevation differences are considered in the formulation of the gust parametrization and the convective gust contribution is adjusted according to the observed climatology.

The presented work advances the understanding of how surface winds change in a warmer climate at high midlatitudes and improves the model forecasting of wind gustiness over Sweden.

Keywords: mean and gust wind speed; stilling-reversal phenomena; regional climate models; climate reanalyses; ERA5; parametrization; NAO; extratropical cyclones; surface roughness; Sweden.

Sammanfattning

En kombination av antropogena aktiviteter och klimatförändringar har under de senaste decennierna lett till en minskning i nära ytvindars magnitud, något som betecknas "stilling" på engelska, och till en mer aktuell återhämtning av denna minskning. Det är viktigt att förstå hur nära ytvindar har förändrats och att identifiera faktorer som driver den observerade variabiliteten, så att lämpliga framtidsscenarier kan skapas. På så sätt är det möjligt att utveckla anpassningsstrategier som ökar samhällets tålighet mot framtida förändringar i vindklimatet. Detta är speciellt viktigt för Sverige, som är mycket sårbar för förändringar i medelvinden och förekomsten av extrema vindar. Den här avhandlingen kartlägger därför variabiliteten av nära ytvindar i Sverige under de senaste decennierna och undersöker vilka mekanismer som driver variabiliteten och de observerade förändringarna. Studien utfördes genom att skapa och använda homogeniserad vinddata baserad på in-situ observationer och genom att analysera aktuella klimatsimuleringar av vindbyar.

Resultaten visar att båda den observerade medelvindens och vinbyns hastigheter utmärks av nonlinjära förändringar under de senaste decennierna, som drivs av den dominanta variabiliteten på vintern. Man kan se i synnerhet att den signifikanta minskningen av vindhastigheter upphördes 2003 och att inga signifikanta trender observerades sedan dess. Detta är konsistent med det observerade omslaget av minskingen i vindhastigheter ("stilling-reversal") på global nivå. Studien pekar dessutom på att det upptäckta omslaget i Sverige är relaterad till förändringar i den storskaliga atmosfäriska circulationen, särskilt till nordatlantiska oscillationen (NAO) och till intensitetsförändringar av extratropiska cykloner som passerar Sverige. Jämförelsen med data från klimatreanalyser visar att, förutom den storskaliga interårliga variabiliteten, förändringar i ytans skrovlighet, till exempel förändringar i skogsytor, har bidragit till de observerade vindförändringarna i Sverige. Därförutom avslöjar avhandlingen att nuvarande regionala klimatmodeller och klimatreanalyser saknar förmågan att simulera historiska vindbyar i Sveriges inlandsregioner och bergsområden på ett adekvat sätt. Simuleringarna förbättras däremot när topografi och altitudsskillnader räknas in i den matematiska formuleringen av vindby- parametriseringen och när vindbykontributionen från konvektiva processer anpassas efter observerade klimatologier.

Den presenterade studien ökar förståelsen av hur ytvindar förändras i ett varmare klimat över de högre midlatituder och ger underlag till att förbättra modellprognoser av vindbyar i Sverige.

List of papers

This thesis is based on the following studies, referred to in the text by their Roman numerals. The published studies are reprinted with the permission from the respective journals.

Appended to the thesis:

I. Safaei Pirooz A. A., Flay R. G. J., **Minola L.**, Azorin-Molina C., & Chen D. (2020): *Effects of sensor response and moving average filter duration on maximum wind gust measurements.* Journal of Wind Engineering & Industrial Aerodynamics, 206, 104354

II. Deng K., Azorin-Molina C., **Minola L.**, Zhang G., & Chen D. (2020): *Global near-surface wind speed changes over the last decades revealed by global reanalyses and CMIP6 model simulations*. Revision submitted to Journal of Climate

III. **Minola L.**, Azorin-Molina C., Guijarro J. A., Zhang G., Son S.-W., & Chen D. (2020): *Climatology of near-surface daily peak wind gusts across Scandinavia: observations and model simulations*. Submitted to Journal of Geophysical Research – Atmospheres

IV. **Minola L.**, Zhang F., Azorin-Molina C., Safaei Pirooz A. A., Flay R. G. J., Hersbach H., & Chen D. (2020): *Near-surface mean and gust wind speeds in ERA5 across Sweden: towards an improved gust parametrization*. Climate Dynamics, 55, 887-907

V. **Minola L.**, Azorin-Molina C., & Chen D. (2016): *Homogenization and assessment of observed near-surface wind speed trends across Sweden, 1956-2013*. Journal of Climate, 29, 7397-7415

VI. **Minola L.**, Reese H., Lai H.-W., Azorin-Molina C., Guijarro J. A., Son S.-W., & Chen, D. (2020). *Wind stilling-reversal across Sweden: The impact of land-use and large-scale atmospheric circulation changes*. Submitted to International Journal of Climatology

Contributions: The selected studies could not become articles in their final stage without the collaborative nature of the research behind them, which is reflected by the co-authorship. In Paper III, IV, V, VI, Minola led the study design, the data analysis and the writing. In Paper I, Minola helped in conceiving the study, he revised the manuscript and approved the final version. In Paper II, Minola initialized the reanalysis comparison, he revised the manuscript and approved the final version.

Other publications not included in this thesis:

Azorin-Molina C., Menendez M., McVicar T. R., Acevedo A., Vicente-Serrano S. M., Cuevas E., **Minola L.**, & Chen D. (2017): Trends of land and ocean trade wind speed in the Canary Islands and surrounding Atlantic Ocean, 1948-2014. *Climate Dynamics*, 50, 4061-4081. https://doi.org/10.1007/s00382-017-3861-0

Azorin-Molina C., Asin J., McVicar T. R., **Minola L.**, Lopez-Moreno J. I., Vicente-Serrano S. M., & Chen D. (2018). Evaluating anemometer drift: A statistical approach to correct biases in wind speed measurement. *Atmospheric Research*, 203, 175-188. https://doi.org/10.1016/j.atmosres.2017.12.010

Azorin-Molina C., Rehman S., Guijarro J. A., McVicar T. R., **Minola L.**, Chen D., & Vicente-Serrano S. M. (2018): Recent trends in wind speed across Saudi Arabia, 1978-2013: a break in the stilling. *International Journal of Climatology*, 38, e966-e984. https://doi.org/10.1002/joc.5423

Zhang G., Azorin-Molina C., Chen D., Guijarro J. A., Kong F., **Minola L.**, McVicar T. R., Son S.-W., & Shi P. (2020): Variability of daily maximum wind speed across China, 1975-2016: An examination of likely causes. *Journal of Climate*, 33 (7), 2793-2816. https://doi.org/10.1175/JCLI-D-19-0603.1

Azorin-Molina C., McVicar T. R., Guijarro J. A., Trewin B., Frost A. J., Zhang G., **Minola L.**, Son S.-W., & Chen D. (2020): A decline of observed daily peak wind gusts with distinct seasonality in Australia, 1941-2016. Submitted to *Journal of Climate*

Table of Contents

Acknowledgements

On 2nd August 2020 Genoa FC had to play its last game in 2019-2020 serie A season: only with a victory the team could avoid the relegation. This was more or less the reflection of coach Davide Nicola the day before this important match…

In or out? Everything or nothing? Yes, it seems to be like this, but, if we reflect little longer, it is not just like that. Of course, we are judged by the results that can arrive or not, but in between there is a precious and meticulous work that can lose value if we do not reach our goals. This can actually sound sad and makes you lose confidence, especially when you are young and at the beginning of the journey to find your place in life. If I lose, I am nothing; if I win, I am the best, the strongest, the most beautiful. It is not surprising if we struggle to accept responsibilities or if it is difficult to like and accept our self. Maybe we should consider that we can be successful only if we consider all our experiences as a process for improving, necessary to build our identity and to get to know what we are able to do. This stands alone from the success or victory we may reach in a given moment. If we are afraid of failure, we avoid taking actions that may lead to the success. But before the success, there is a long list of unsuccessful attempts. Let's then risk and accept to fail because at the end failure is just an attempt to reach our goal. And this attempt is the most important and honorable action, even greater than reaching the goal or the success itself. Tomorrow I will not feel more capable if I will win, or incompetent if I will lose. I am aware that I can win or lose, but I am more aware of the journey done to reach a destination and just this make me a winner.

It the same way, this thesis is the result of 5 years of work, but it cannot explain alone what these past years mean to me. Here I want to thank everyone who was part of this journey and help me in writing this thesis.

I would like to thank my supervisor Deliang Chen for giving me the opportunity to start this adventure. Even with its busy schedule, he was always there to give me direction in the most crucial moments of my Ph.D. studies. He taught me a lot with his experience and knowledge, showing me how to deal with the pressure and the disappointments that research makes you face.

I am greatly thankful to my co-supervisor Cesar Azorin-Molina. He was always there to support me in every single step of this thesis, and he helped me anytime I needed assistance or advices. In particular, he proved me what can be achieved with the hard work and passion.

I also would like to thank my mentor Julia Grönros who helped me in discovering all the opportunities I can find when my Ph.D. studies will end. She gave me a lot of tips for my studies and she showed me how life and work can find perfect balance.

This thesis would have not been possible if I would have not met Fuquing Zhang. During my stay at Penn State University, he made me believe that I could reach great results with my hard work. Unfortunately, he left too early and he cannot see the outcomes of our collaboration.

I wish to thank Roland Barthel for being my examiner. Even if the past months were a difficult time for him, he did not give up to his examiner duties and he guided me to the conclusion of my studies.

I am greatly thankful to all my colleagues at the Regional Climate Group and at the Department of Earth Sciences for their friendship and support. They were all a source of inspiration for the idea behind the results presented in this thesis. A special thanks to Julia Kukulies who helped me with the "sammanfattning" and read carefully this thesis. I also would like to thank Ezra Haaf and Michelle Nygren for the hours spent together in our writing sessions. A great thanks to Aifang Chen and Ezra Haaf who helped me in finding direction in the deadlines jungle I experiences in the past months.

A special thanks to all the researchers around the world that collaborated with me during the past years. It has been amazing to learn from them by working as a team. This thesis would have not been possible without their precious and meticulous work.

My deepest gratitude is for all the friends I had here in Gothenburg during the past years. I enjoyed research also because I had them waiting for me outside the working hours. A special thanks to Giovanni Dufour, Andrea Amodeo, Chiara Rinaldi, Andrew Nisbet, Sara Pedri and Robert Stewart for looking after me especially during these last few months, where so much was passing in front of me, so much work was making me blind, but they were there saying to me that I could deal with everything.

I managed to conclude this thesis also thanks to Corrado Motta. He saw and understood all my struggles, making me notice how much I was achieving meanwhile. These last months of writing were much easier also thanks to all the fun activities we did together at the Happy Lägenhet.

I must mention all the true friendships that I had the chance to grow in the past years and gave me so much. Everything I learn thanks to my friends, in a way on the other, has helped me to write this thesis. Even if few friends may be far away or with few of them I have less contact now, they have all been an important part of this experience and I am thankful that they shared with me a part of their life.

In the last years, I risked and accepted to fail also thanks to my childhood friends Federico Albertini, Andrea Bonsignori and Filippo Caccia. When I am around them, life always seems so easy. Besides, I learned from them the determination I proved in the last months. I am so grateful to have them in my life.

These past years were not always easy, and I often discover myself standing scared and lost in front of the challenges I had to face. In these times, when I found myself hopeless and I thought that the fire inside of me was dying out, two persons were always there to keep my sparks alive: my mother Silvia and my sister Linda. They were able to support me in all the paths I decided to take, and, even if they were far away, I always found them there waiting for me and trusting me. What I achieved in the last years and with this thesis is also because I have them by my side.

Lorenzo Minola, Gothenburg in October 2020

PS, Genoa won 3-0 against Hellas Verona on 2nd August 2020, avoiding the relegation for the second year in a row thanks to the result in the last league match.

List of abbreviations

ABL	Atmospheric Boundary Layer
AWS	Automatic Weather Station
CMIP5	Coupled Model Intercomparison Project Phase 5
CMIP6	Coupled Model Intercomparison Project Phase 6
CPM	Convection-Permitting Models
DAWS	Daily Average mean Wind Speed
DPWG	Daily Peak Wind Gust
ECMWF	European Center for Medium-Range Weather Forecasts
Euro-CORDEX	Coordinated Regional Downscaling Experiment across Europe
GCM	General Circulation Model
GF	Gust Factor
GHG	Greenhouse Gases
NAO	North Atlantic Oscillation
NH	Northern Hemisphere
PDO	Pacific Decadal Oscillation
R	Gust Factor Ratio
RCM	Regional Climate Model
RMSE	Root Mean Square Error
SH	Southern Hemisphere
SMHI	Swedish Meteorological and Hydrological Institute
SNHT	Standard Normal Homogeneity Test
SST	Sea Surface Temperature
WG	Wind Gust
WGE	Wind Gust Estimate
WMO	World Meteorological Organization
WS	Mean Wind Speed

1 Introduction

1.1 The impact of near-surface winds

Near-surface wind plays a crucial role in the transfer of heat, moisture, energy and momentum between the Earth's surface and the atmosphere (Abhishek et al. 2012). Humans rely on wind when it comes to electricity production from wind farms, which is a still growing green energy sector (REN21 2020). By governing the evaporation demand, surface winds partly control agriculture productivity and can strongly alter the hydrological cycle (Rayner et al. 2007; McVicar et al 2012a, 2012b). Wind speed conditions greatly affect the accumulation and dispersion of air pollutants near emission sources such as traffic in urban areas, even in the top-ranked sustainable city of Gothenburg (Grundström et al. 2011; Grundström et al. 2015; Global Destinations Sustainability Movement 2019).

The occurrence of extreme winds has even more evident impacts on the environment and the society. It can affect aviation security, as well as damage buildings and forests, representing a severe hazard to people, properties and transport (Achberger et al. 2006; Suomi et al. 2014). Worldwide, storms with their associated strong winds and rainfall have been identified as the costliest among various type of climate-related and geophysical disasters, with twice the reported losses for either floods or earthquakes (Walemacq et al. 2018). Across Europe, windstorms and strong winds contribute to more than half of the economic losses associated with natural disasters (Ulbrich et al. 2013). In Sweden, where forests cover 56% of the land and 95% of those forests being used in the timber industry, wind damages can seriously affect the national economy (Hannon Bradshaw 2017). For example, storm Gudrun in 2005 fell with its strong wind gusts (i.e., sudden and brief increase in wind speed) about 75 million m^3 of trees just in Sweden, which equal the normal annual harvest of the whole country (Haanpää et al. 2007). In addition, falling trees caused severe damages to the power supplies, telecommunication networks, roads, and railways (Swedish Commission on Climate and Vulnerability 2007). 17 people lost their life, and the direct costs reached SEK 21 billion.

For all the mentioned reasons, it is crucial to understand how near-surface winds are likely to change in a warmer future. The most harmful effects can thus be reduced by adapting the society to the expected new scenarios (IPCC 2014).

1.2 Winds in a changing climate

Traditionally, climate change research has focused on increasing in air temperature and redistribution of precipitation patterns. Only over the last few decades, multidecadal changes in observed near-surface mean wind have been investigated, reporting a general slowdown in terrestrial winds, named "stilling" - term introduced for the first time by Roderick et al. (2007). Such general decrease in near-surface mean winds is observed over land in most northern midlatitude regions in the last ~30-50 years (McVicar et al. 2012a), and it differs from the opposite increasing trends in wind speed revealed over large parts of oceans, especially in the Southern Hemisphere (Tokinaga & Xie 2011; Young & Ribal 2019). Moreover, the Northern Hemisphere near-surface mean winds have shown a recovery in their decline during recent years (Kim & Paik 2015; Azorin-Molina et al. 2018a; Zhang & Wang 2020). In fact, based on in situ observations, Zeng et al. (2019) showed that the break in the land stilling across Northern Hemisphere, especially over Europe, East Asia and North America, became prominent since around 2010.

However, what causes the ocean wind increase, the terrestrial stilling and its reversal is still unclear, even though different possible causes have been proposed. Vautard et al. (2010) attributed a large part of the terrestrial stilling to the increase in surface roughness (e.g. land use changes, forest growth, urbanization). But Zeng et al. (2018) argued that the land greening (i.e. the increase in vegetation cover) had a limited impact on the reduction of terrestrial winds, which implies that there should be additional physical drivers that modulate the changes in global surface winds. Many studies proposed large-scale atmospheric circulation as the key driver in modulating wind speed changes (Wu et al. 2018). In fact, as air temperature increases in a warming climate, it can affect surface pressure gradients and therefore circulation patterns. Large-scale atmospheric circulation changes follow the variation of regional pressure gradients, which vary as the result of regional warming differences (Lin et al. 2013). For example, the reversal in terrestrial stilling has been proposed to be linked to the phase change in the North Atlantic Oscillation (Azorin-Molina et al. 2018a) and the Pacific Decadal Oscillation (Zeng et al. 2019). Besides, the aging of measuring instruments can also lead to a slowdown of observed near-surface wind speed (Azorin-Molina et al. 2018b).

Driven by the twenty-century surface air temperature rise, extreme winds could also change in their frequency and magnitude of occurrence (Azorin-Molina et al. 2016). Even so, the understanding about a theoretical connection between warming climate and increase in the intensity and frequency of wind extremes is still weak (Vautard et al. 2019). Most recent studies have mainly focused on the terrestrial mean wind speed, with only few studies of extreme wind speed, as wind gust (Wu et al. 2018). For instance, a slowdown in wind speed extremes were reported across Europe [e.g., Netherlands (Cusack 2013), Spain and Portugal (Azorin-Molina et al., 2016), Czech Republic (Brázdil et al. 2017)], which does not agree with the increase documented for Japan (Fujii 2007) and the United States (Klink 2015). In fact, due to the possibility of a change in the wind speed distribution, there is no consensus about trends of wind extremes relative to the mean. In-depth extreme wind analyses are thus necessary by improving observation of extreme (and gust) winds to investigate their spatio-temporal characteristics and potential causes of changes (Wu et al. 2018).

One of the main reasons limiting the study of observed near-surface wind series is the uncertainty about the reliability of in-situ measurements (Azorin-Molina et al. 2014). In particular, various sources of artefacts can affect wind measurements consistency. Additionally, multidecadal wind measurements are often lacking since systematic measurements (especially of extreme and gust wind observations) have been carried only in the last few decades (see Section 3.2). So far, wind investigations have mainly focused on midlatitude areas where the majority of near-surface wind observations are available (McVicar et al. 2012a). This contrasts with the fewer number of studies for high latitudes in the Northern Hemisphere such as Canada (Wan et al. 2010) and Alaska (Lynch et al. 2004; Hartmann & Wendler 2005). Indeed, there have been no such studies dealing with multidecadal variability of observed near-surface mean and gust wind speed for such high latitudes in Europe.

1.3 The need of modelling wind

Because reliable wind observations are not always accessible or not easy to interpret, alternative datasets like climate reanalyses and models should be used for understanding how the changing climate affects wind.

Reanalysis datasets, with their complete spatial coverage and consistent temporal resolution (Dee et al. 2011), have been extensively used in the literature to describe and explore near-surface mean wind speed changes in the past decades (e.g. Torralba et al. 2017). Their reliability in representing near-surface mean wind speed has been largely explored using in-situ observations. Results show that their capability in representing observed near-surface mean wind speed variability is strongly dependent on the selected region and the considered time period (Ramon et al. 2019; Wohland et al. 2019; Yu et al. 2019; Miao et al. 2020). But when it comes to the ability in representing surface wind gusts, their skills are still largely unknown.

In addition to reanalyses, climate models can be used to simulate wind statistics under different climate projections, by setting the forcing to change according to a possible future scenario (Collins et al. 2013). In particular, Regional Climate Models (RCMs), with their regional refinements, can quantify possible changes in wind extreme (as gust) statistics under different future projections (Nikulin et al. 2010; Jeong & Sushama 2019). Thanks to their resolution scale comparable to the one used in most impact assessments, RCMs provide a primary tool for the development of risk management strategy or adaptation policy.

However, before any climate model or reanalysis dataset can be used to assess changes in extreme winds, its ability in representing observed near-surface wind statistics (such as gusts) must be proven. Their capability in realistically simulating gust wind speeds must be investigated using observations, as done by Kunz et al (2010) for Germany. Unfortunately, there are currently no suitable wind gust observational datasets for Sweden that can be used to verify RCMs and reanalysis outputs (Nikulin et al. 2010), and the reliability of available model datasets in simulating extreme wind remains largely unknown (Achberger et al. 2006).

1.4 Objectives

Given the evident vulnerability of Sweden to surface winds and keeping in mind the framework of the widespread terrestrial wind stilling and recent reversal, this thesis aims at investigating near-surface mean and gust wind speed variability across Sweden. So far, no comprehensive research has been done in regards to near-surface winds for Sweden using multidecadal in-situ measurements.

In particular, after investigating what drives mean wind speed variability at a global scale, this thesis focuses on Sweden. First, high-quality and homogenized datasets of observed near-surface mean and gust wind speed are created for the longest-available time period. Afterwards, the observed wind gust dataset is used to evaluate if current RCMs and reanalyses have adequate skills in simulating wind gustiness and to further improve how wind gusts are modelled (parametrized). Last, changes in the created observed wind datasets are investigated to assess what drives their past variability and to understand what could be their plausible changes in the future.

To summarize, the five objectives of this thesis are:

1) to investigate past global changes in near-surface wind speed through the use of climate models and reanalyses (Paper II)

2) to create the longest available datasets of observed near-surface mean and gust wind speeds for Sweden (Paper V & Paper VI).

3) to investigate the impact of the different gust duration adopted to measure surface wind gusts across Sweden (Paper I).

4) to evaluate the performance of RCMs and reanalyses in simulating near-surface wind gust over Sweden (Paper III & Paper IV).

5) to estimate past variability in near-surface mean and gust wind speeds across Sweden in relation to global wind changes and to identify the possible causes behind the observed changes (Paper V & Paper VI).

2 Drivers of surface wind variability

2.1 What drives near-surface wind changes?

If we want to understand how near-surface winds vary over the years, we must first identify the mechanisms that drive wind changes. Wind is generated by pressure gradients and modified by friction and the Coriolis force due to Earth's rotation (Zhang et al. 2019). From a dynamical perspective, the motion in the atmosphere can be expressed by the Lagrangian form of the wind equation (Wu et al. 2018):

$$\frac{\mathrm{d}\vec{\mathrm{V}}}{dt} = \vec{G} + \vec{F} + \vec{g} + \vec{f} \qquad (1)$$

where:

- $\vec{\mathrm{V}}$ is the wind speed.
- $\vec{G} = -\frac{1}{\rho}\nabla p$ is the pressure gradient force, which is the driving force for atmospheric motion; ρ and p are the air density and air pressure, respectively.
- $\vec{F} = -2\vec{\Omega} \times \vec{\mathrm{V}}$ is the Coriolis force, the inertial force that has to do with the rotation of the Earth.
- $\vec{g}$ is the gravitational force.
- $\vec{f}$ is the frictional or drag force.

Therefore, Equation 1 shows that changes in near-surface wind speed can be driven by changes in the driving force and/or in the friction component.

Pressure gradient varies driven by the dynamic (circulation patterns) and thermodynamic forcing (e.g., temperature gradient) (Landberg 2016; Wehrli et al. 2018). The dynamic component generally refers to the circulation-induced influences, which range from geostrophic wind, weather regimes, and overall large-scale circulation patterns to local wind. The thermodynamic component includes phase transitions, differences in lapse rate and land-sea contrast as well as effects from the partitioning of radiative and turbulent fluxes (e.g., thermals).

The frictional force can be split into the surface friction force (due to the damping effect of surface roughness) and the turbulent friction force (due to turbulent dissipation within the boundary layer) (Zhang et al. 2019). Thus, changes in the frictional components can be induced by changes in the atmospheric stability or in changes of surface roughness associated with factors such as urbanization, forest growth or clear cutting, desertification, changes in trees and forest distribution or changes in agricultural practices (Yupeng et al. 2019).

2.2 Geographical controls on surface winds across Sweden

Sweden is located in northern Europe, occupying the eastern part of the Scandinavian Peninsula. It extends over a total area of about 450000 km^2 along a distance of 1574 km, crossing ~14° of latitudes (from ~55°N to ~70°S). More than half of the country boundaries are coastlines, which include several small islands and reefs, especially in the east and southwest. The topographic features of Sweden are shown in Figure 1. The north-to-south mountain range of the Scandes dominates central and northern Sweden, along the Norwegian border and in the country inland above 58°-60°N. Scandes slope down to lowlands and plains in the east and south-east. Most of the rivers flow southeast from the Scandes mountains to the Gulf of Bothnia, creating numerous river valleys in the northwest-southeast direction. Numerous lakes, by lying in these river valleys, result in having a common northwest-to-southeast elongated shape.

Winds over Sweden are generally dominated by those from westerly and southwesterly directions, driven by the interannual fluctuations in the strength of the Icelandic low and the Azores high, measured by the North Atlantic Oscillation (NAO) index (Jönsson & Fortuniak 1995; Chen 2000; Hanssen-Bauer & Førland 2000). Surface winds across Sweden are also controlled by the cyclonic and anticyclonic circulations over Europe (Chen 2000; Achberger et al. 2006), in particular cyclones developed over the arctic and polar fronts (Martyn 1992). In the eastern region of the Scandes, the numerous valleys in the northwest–southeast direction partly force winds to follow the valley orientation (Achberger et al. 2006). The absence of mountain sheltering in the west of the southern region exposes the area to westerlies (i.e., winds from the west or southwest directions; Jönsson & Fortuniak 1995). Local wind systems (i.e., sea breezes and local winds) can develop from the long-extended coastline regions, the numerous lakes, or the Scandes topography, but the stronger regional winds overcome these local winds during most of the year (Borne et al. 1998; Achberger et al. 2006).

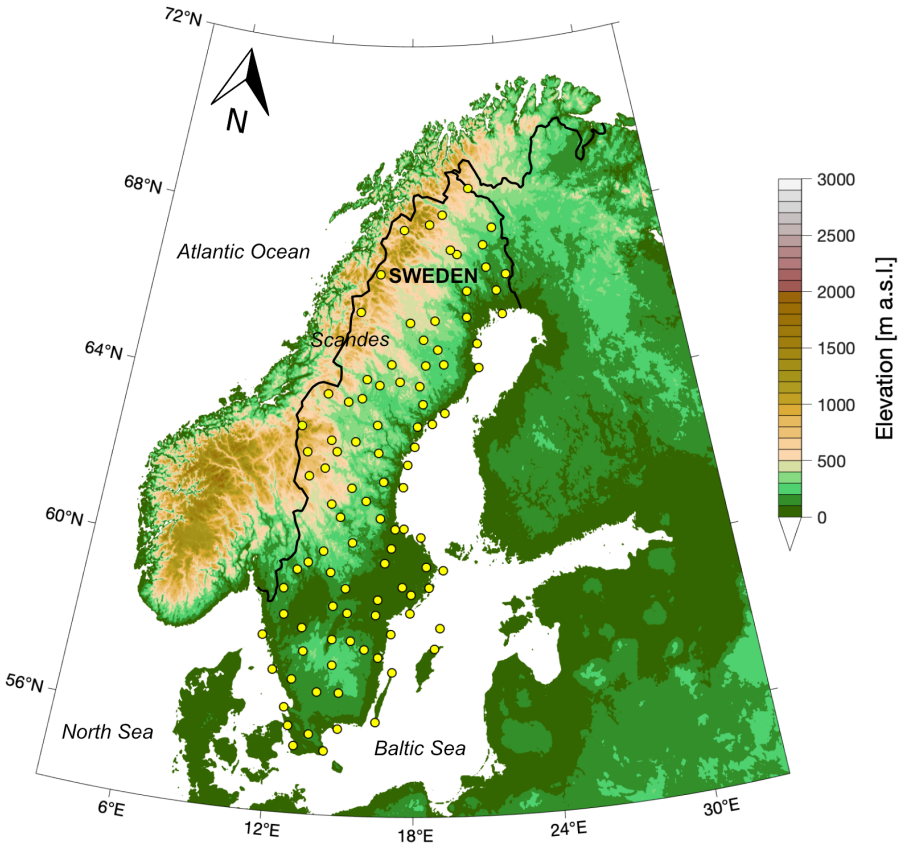

Figure 1. Elevation map of Sweden (and surrounding) with the location of the 100 weather stations used in this thesis (yellow circles) (Figure 1 from Paper VI)

3 Measurements and data homogeneity

3.1 What do we measure?

Surface wind observations are needed for weather monitoring and forecasting, for wind-load climatology, for estimating wind damages and wind energy, for calculating surface fluxes (e.g. air pollution dispersion), etc. (WMO 2014). As wind speed increases considerably with height, in particular over rough terrain, a standard height of 10 m above an open terrain is recommended by the World Meteorological Organization (WMO) for the exposure of wind instruments when it comes to measure near-surface winds. In a wind-measuring system, a sensor (e.g. cup and ultrasonic anemometers) records wind in its variations in speed over time through the generation of a high-frequency (e.g. 0.25 s) signal. For example, in a cup anemometer, such signal is created as the angular velocity of the cup is designed as directly proportional to the wind speed. The generated high-frequency signal is then processed (i.e. averaged) by the processing system paired to the sensor, in order to deal with the extremely turbulent signature of the atmospheric flow (Landberg 2016). WMO recommends to record near-surface mean wind speed (hereafter, WS) as the mean wind speed over the last 10 minutes in a specified time interval (i.e. 10 m averaged time of the high-frequency signal; see Figure 2) (WMO 2014). With hourly weather reports, WS refers to the mean wind in the last hour.

To define the occurrence of extreme wind events, just looking at the near-surface WS with its 10 min averaged interval is not sufficient. To capture the abrupt increase in wind and its turbulent signature, WMO suggests to also record the so-called near-surface (~10 m height) peak or wind gust (hereafter, WG), defined as the maximum 3 s wind speed over a specified time interval (WMO 1987). With hourly weather reports, WG refers to the wind extreme in the last hour. By definition, WG can capture the turbulent fluctuations due to the short averaging time of the wind speed calculation (Figure 2), and can provide complementary information to WS climatology, particularly for determining the occurrence of severe wind events. Among the several definitions of gust, WMO adopted the 3 s moving average gust speed definition because it was generally believed that the effective gust duration of earlier generation analogue wind-measuring systems was approximately 2-3 s, which was the basis of the gust definition in many wind-loading standard (Kwon & Kareem 2014).

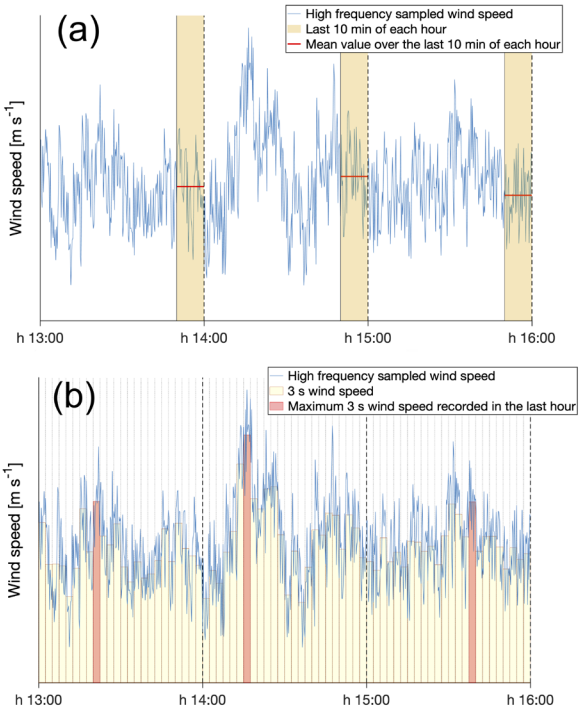

Figure 2. Example of how a high-frequency sampled signal is processed to generate (a) hourly mean and (b) gust wind observations.

In order to better understand what is included in WG measurements in addition to what already WS records, we can refer to the Reynolds decomposition (Landberg 2016). Mathematically, a time series, as a wind series, can be written as:

$$V = \bar{V} + V' \quad (2)$$

where V is the wind speed, $\bar{V}$ the mean, and V' is what remains when the mean wind speed has been subtracted, that is the turbulence (by assuming that the time series is stationary and there are no trends). When looking at WG measurements with the lens of the Reynolds decomposition, we can rewrite Eq. (2) as:

$$WG = WS + \max(turbulence) \quad (3)$$

where max ($turbulence$) include additional turbulence that is not included in the 10 min averaged duration of the WS definition. In particular, it refers to those strong turbulent eddies which time scale cannot be captured by a 10 minutes wind signal processing, and only a shorter averaged time of 3 s can detect. For example, the most damaging turbulent eddies are those that engulf an entire building and have a dimension of the order of the size of this structure (WMO 1987). In many cases this has the order of 100 m. With strong winds, this implies that the gust duration is of the order of few seconds. Therefore, such damaging gusts can be detected in wind measurements by only including the max ($turbulence$) term in the WG definition of Eq. (3).

Turbulence in the atmosphere is generated through two physical mechanisms (Landberg 2016; NOAA 2018):

- Mechanical
- Thermal (convective)

Mechanical-generated turbulence results from the friction between the air and the ground, especially if the flow is crossing irregular terrain and/or buildings. Such friction causes strong shear near the surface: in fact, the wind velocity at the surface is zero and then it increases as it gets further and further away – this generates shear in the flow and turbulent eddies, whose intensity depends on the strength of the surface wind, the nature of the surface and the air stability.

Thermal turbulence is associated to warm days when the sun unevenly heats the Earth's surface (certain surfaces are heated more rapidly than others). The result is that isolated convective currents are set in motion by warm air rising and cooler air descending. This process can be quite violent, with convective currents often strong enough to produce air mass thunderstorms with which severe turbulence and gusty winds are associated.

3.2 Wind observations across Sweden

Near-surface wind measurements across Sweden are provided by the Swedish Meteorological and Hydrological Institute (SMHI). All the meteorological observations are available online at the SMHI open data page (https://www.smhi.se/data/utforskaren-oppna-data/).

Near-surface WS is defined as the mean wind over the last 10 min, following the WMO (2014) output-averaged time instructions. WS was measured with either cup anemometers or a Thies ultrasonic anemometer 2D. Before 1995, WS was measured with the Söderlund mechanical cup anemometers located on lighthouses or at airport meteorological stations (Achberger et al. 2006). WS measurements were mostly recorded every 3 h and concentrated along the coastline and in southern Sweden. In 1996 SMHI started to install about 120 automatic weather stations (AWS) across the country, all equipped with the Thies ultrasonic anemometer 2D placed at the standard height of 10 m above the ground (Wern & Bärring 2009). At the AWS measurements have been made every hour. Alexandersson (2006) reported that across Sweden most stations measured WS at the standard height of 10 m during 1961-2004, with the exception of some coastal stations where anemometers were located at the top of hills and rocky islands. In this way, measuring height of coastal stations ended up to be often higher than 10 m. Only after 1996, with the new installed AWS, the wind-measuring network used identical anemometers at the same standard height of 10 m (Wern & Bärring 2009).

Systematic WG measurements are available only since the end of the 1990s, when SMHI started to install the new AWS. WGs were measured at 10 m height as the maximum 2 s gust recorded in the last hour (S. Lekander 2019, personal communication), which differs by 1 s from the standard 3 s averaging time suggested by WMO (2014).

In the various Papers included in this thesis, observed WS and WG series are analyzed as:

- Monthly averaged WS series – Paper V
- Hourly WS and WG series – Paper IV
- Daily Average mean Wind Speed (hereafter, DAWS) series, i.e. the mean WS recorded in 24 h – Paper VI

- Daily Peak Wind Gust (hereafter, DPWG) series, i.e. the highest WG recorded in 24 h (Azorin-Molina et al. 2016) – Paper III and VI

3.3 The impact of a different gust duration

As previously mentioned, WG is measured across Sweden by employing a 2 s gust duration, which differs by 1 s to the WMO recommendation (3 s). For this reason, it is necessary to understand the effect of using a different moving average filter duration (2 s instead of 3 s) on the recorded maximum gust wind speeds. This is investigated in Paper I.

For this purpose, a series of wind-tunnel experiments are carried out using a cup anemometer under different turbulent intensities, and the wind-tunnel results are compared with values computed from the theoretical approach of the random process and linear system theory (Davenport 1964). In particular, the comparison between 2 s and 3 s gust speeds is done through the use of the gust factor (GF), defined as:

$$GF = \frac{\widehat{U}}{\overline{U}} = 1 + g \cdot \frac{\sigma_u}{\overline{U}} \qquad (4)$$

where $\widehat{U}$ is the gust speed, g is the peak factor, σ_u is the standard deviation of the along-wind speed fluctuations about the mean wind speed during period T, and $\overline{U}$ is the mean speed. In addition, the ratio between the GF for different gust durations, called gust factor ratio (R), is also analyzed:

$$R = \frac{GF_{d1}}{GF_{d2}} \qquad (5)$$

where d1 and d2 are shorter (2 s) and longer (3 s) gust durations, respectively. The error ε is also defined to quantify the difference in GF at two different gust durations:

$$\varepsilon = \frac{GF_{d1} - GF_{d2}}{GF_{d1}} \cdot 100 \qquad (6)$$

Figure 3 shows how the fluctuations of the recorded high-frequency (0.25 s) wind speed signal is smoothed when a moving average filter is applied. All the peaks, both the maximum and the minimum wind speeds, are reduced with the increase in the applied gust duration. Therefore, it is evident that increasing the gust duration from 2 s to 3 s decreases both the gust and peak factors, meaning that lower gust wind speeds are recorded when using a 3 s gust duration compared to the shorter 2 s one.

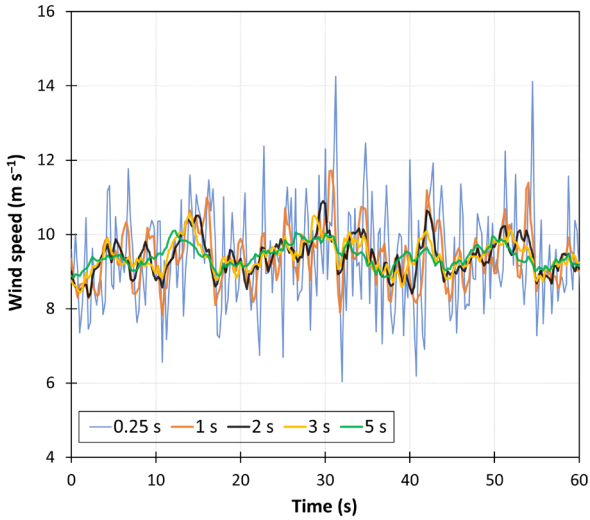

Figure 3. Effect of applying a moving average to the wind speed time series recorded by a WAA151 anemometer in a turbulent wind with turbulent intensity (I_u) = 32.4% and mean wind speed ($\overline{U}$) = 10.1 m s^{-1} (modified Figure 6 from Paper I).

Figure 4 further quantifies the effect of the filtering caused by employing a 2 s or a 3 s moving average. At high turbulence intensities (37%), R and ε drop to around 1.016 and 1.5%, respectively. This means that at high turbulence intensities, 3 s gust speeds are about 4% lower than 2 s gust speeds, given the same incoming flow. Differences are greater for higher turbulence intensities compared to lower ones.

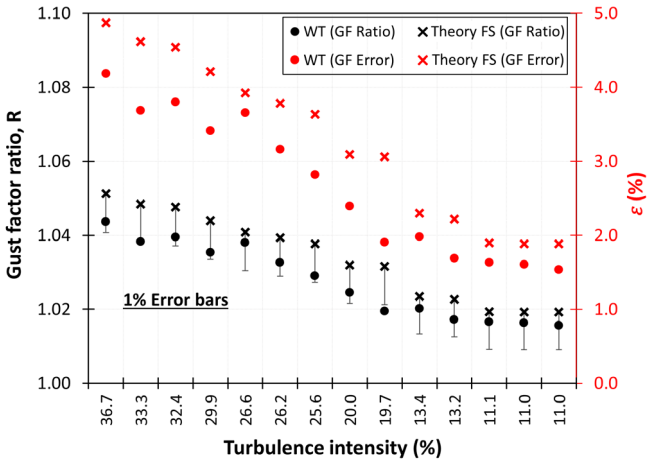

Figure 4. Gust factor ratios (Equation 5) and errors (Eq. 6) between 3 s and 2 s gusts (modified Figure 9 from Paper I).

To conclude, decreasing the effective gust duration (e.g., from 3 s to 2 s) increases both the gust and peak factors, resulting in an overestimation of maximum gust speeds and an underestimation of minimum gust speeds. Similar to the GF differences shown in Figure 4, at high turbulence intensities, the recorded WG speeds differ by 3% - 7% between 3 s and 2 s gust durations, and at low intensities the differences decrease to 1% - 3%.

3.4 Homogenization

A climate time series is homogeneous when its changes are only caused by variations in climate (Aguilar et al. 2003). Only homogeneous time series should then be considered in studies dealing with multidecadal changes in climate. Unfortunately, long-term climatological series can be affected by various non-climatic factors which make these data unrepresentative of the actual climatic variation occurring over time. Sources of inhomogeneities in long-term near-surface wind series can be related to:

- station relocation and anemometer height changes (Wan et al. 2010)
- changes in instrumentation (i.e. anemometer type) and/or measuring practice (e.g., use of different sampling intervals) (Pryor et al. 2009; Azorin-Molina et al. 2014)
- instrument malfunctions (e.g., degradation of the instrument performance) (Azorin-Molina et al. 2018)
- changes in the environment surrounding the monitoring station (e.g., changes in the exposure of the observing site) (Aguilar et al. 2003)

Figure 5 shows how an inhomogeneous series looks like. Karlstad Flygplats station (from Paper V) was relocated in 1997, and such relocation caused an artificial drop in the annual mean wind speeds recorded.

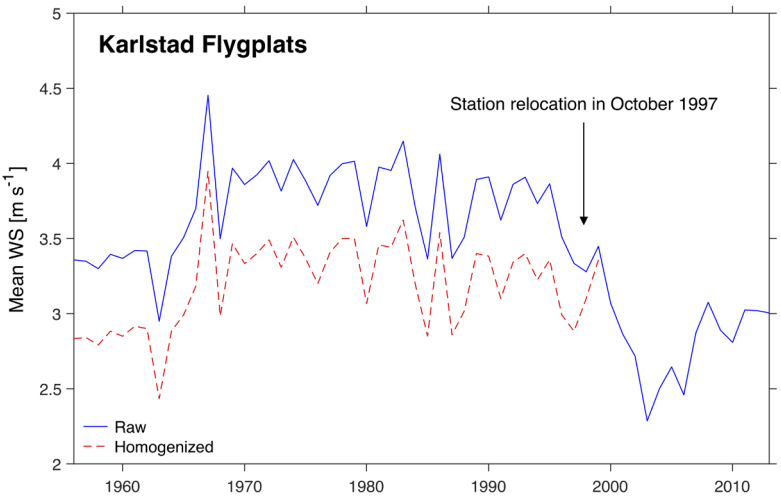

Figure 5. Raw and homogenized annual mean wind speed series of Karlstad Flygplats, 1956-2013.

A homogenization protocol must be applied to identify possible artificial shifts (or break-points) and afterwards remove the biases which those inhomogeneities create (Aguilar et al. 2003; Wan et al. 2010). To achieve this, a reference time series should be compared to the station to be homogenized. The reference series should be homogeneous and have the same climatic signal of the candidate series (i.e., it should have experienced all the general climatic influences of the base series, except its artificial biases).

Part of the objectives of this thesis is to create observed near-surface wind datasets for Sweden. In particular, this study aims:

- to obtain high-quality multidecadal (1956-2013) near-surface WS series for Sweden by applying a robust data processing protocol (quality control, reconstruction, homogenization) (Paper V);

- to create the longest available (1996-2016) dataset of homogeneous and complete DPWG observations across Sweden (Paper III);

- to produce the newest and longest available time period (1997-2019) with homogeneous DAWS and DPWG series across Sweden (Paper VI).

In Paper V monthly mean wind speed series are homogenized using monthly mean series of geostrophic wind as reference series, following Wan et al. (2010). Geostrophic wind series represent suitable reference series because (i) winds in Sweden are controlled much more by large-scale synoptic systems (i.e., pressure gradient forces) than by local thermal gradients (Jönsson & Fortuniak 1995; Borne et al. 1998; Achberger et al. 2006), and (ii) complex topography (except for the western part of the country) is not a feature of the surface roughness in Sweden (Achberger et al. 2006). By using the *AnClim* software (http://www.climahom.eu/software-solution/anclim) developed by Stepanek (2004), the Alexandersson's standard normal homogeneity test (SNHT; Alexandersson 1986) is used for detecting inhomogeneities. In particular, SNHT is applied on a monthly basis using the respective geostrophic wind series as reference for each station. *AnClim* detects all the possible inhomogeneities at a statistically significant level of 5%, but these breakpoints are homogenized only when metadata are available, informing for example of a change in station location. In case of no metadata available, they are corrected only when they occur for different months around the same year. Afterwards, wind speed series are adjusted by applying the amount of change before the detected inhomogeneity, assuming that the most recent wind speed measurements are more reliable.

Instead, in Paper III and VI, *Climatol* (Guijarro 2017) is used to perform homogenization and data infilling of the raw wind series. *Climatol* is a R (R Core Team 2020) package designed for quality controlling, homogenizing and infilling climate series (further information are available at https://www.climatol.eu/). By working with "normalized" values (normalization of a time series is achieved through division by the series average), *Climatol* performs homogenization using a two-step iterative approach (Guijarro 2018):

1) In step 1, reference series are calculated by averaging their 5 closest series at each time step, and break-points are identified by applying the well-established SNHT test to the differences between the observed and the calculated "normalized" values, at two different stages: (i) on stepped overlapping time windows, to minimize the possible masking effect of multiple break-points; and (ii) on the whole series. Break-point finding is repeated iteratively until no SNHT values higher than the specified thresholds are detected.

2) In step 2, once all break-points are identified and corrected, missing values are filled by means of the 5 closest observations, weighted by an inverse distance function.

The advantage of using *Climatol* compared to the approach used in Paper V is that *Climatol* is able to automatically homogenize a large number of wind series, without needing site metadata, that often is not available (Azorin-Molina et al. 2019). Furthermore, daily time series can be homogenized without performing monthly correction. *Climatol* has been widely applied to homogenize wind series in previous studies (Azorin-Molina et al. 2016; Shi et al. 2019; Azorin-Molina et al. 2019; Zhang et al. 2020). For this reason, *Climatol* is chosen to perform the homogenization of wind series across Sweden in both Paper III and VI.

Notice that in Paper IV hourly wind series are selected for the 5-year period 2013-2017. During this time almost all recorded WS and WG values were quality controlled and ensured by SMHI – no homogenization is therefore needed.

4 Modelling

4.1 Near-surface wind gust parametrization

Numerical models are not able to resolve explicitly those processes with scales of motion smaller than the grid-scale. For this reason, it is necessary to relate the cumulative effects of these subgrid-scale processes to the resolvable scales of motion using the given scale variables. This approach is named parametrization (Anthes 1985). In current models, eddies of all scales responsible for gusts cannot be resolved explicitly and WG is thus parametrized.

Several types of gust parametrization methods can be found in the literature (Sheridan 2011). Given that a gust factor is defined as the ratio between the gust wind and the mean wind speed (Suomi et al. 2013), the simplest way to parametrize gust consists of creating a table of mean gust factors categorized by surface type (UK Met Office 1993). Another method to parametrized gust consists in creating empirical formulas to relate maximum WG to mean daily WS (Weggel 1999). Unfortunately, similar empirical equations depend on the location of where such formulation is derived and there is no reason to believe that this formula is universal.

Fully based on physical consideration, the Wing Gust Estimate (WGE) method of Brasseur (2001) assumes that surface gusts result from the deflection of air parcels flowing higher in the boundary layer, which are brought down by turbulent eddies. Therefore, the WGE estimates wind gusts by considering the deflection of air parcels travelling at a given height, which are able to reach the surface when the mean turbulent kinetic energy of large turbulent eddies is greater than the buoyant energy difference between the surface and the height of the parcel.

Another common method to parametrize gust is based on the work of Panofsky et al. (1977) and Bechtold & Bidlot (2009). This parametrization technique is for example used in the current reanalysis products of the European Center for Medium-Range Weather Forecasts (ECMWF), as ERA5 (see Section 4.2.3). Wind gusts are parametrized and calculated post-processing (ECMWF 2016) with the parameter gust (hereafter, GUST) computed at each model integration step. Its maximum since the previous post-processing time is written out and archived as WG. The gust parameter gust is calculated at each time step of the model as the sum of three terms:

$$\mathrm{GUST} = \mathrm{WS}_{\,\mathrm{instantaneous}} + \Delta\mathrm{WG}_{\,\mathrm{turbulent}} + \Delta\mathrm{WG}_{\,\mathrm{convective}} \qquad (7)$$

where, $\mathrm{WS}_{\,\mathrm{instantaneous}}$ is the instantaneous 10 m wind speed, $\Delta\mathrm{WG}_{\,\mathrm{turbulent}}$ is the turbulent gustiness, and $\Delta\mathrm{WG}_{\,\mathrm{convective}}$ is the convective contribution.

$\Delta\mathrm{WG}_{\,\mathrm{turbulent}}$ expresses the gustiness driven by the shear-stress (function of the friction velocity) and the stability of the boundary layer (function of the Monin-Obukhov length) and its formulation was derived by the field experiments of Panofsky et al. (1977) over uniform surfaces and based on the similarity theory (Arya 2001). It is calculated as:

$$\Delta\mathrm{WG}_{\,\mathrm{turbulent}} = \mathrm{C}_{\,\mathrm{turbulent}} \cdot \Delta\mathrm{WG}_{\,\mathrm{friction+stability}}$$

$$= \mathrm{C}_{\,\mathrm{turbulent}} \cdot \mathrm{u}_{*} \cdot \mathrm{f}\left(\frac{\mathrm{z_i}}{\mathcal{L}}\right) \qquad (8)$$

with

$$\mathrm{f}\left(\frac{\mathrm{z_i}}{\mathcal{L}}\right) = \begin{cases} \left(1 - \frac{0.5}{12} \cdot \frac{\mathrm{z_i}}{\mathcal{L}}\right)^{1/3} & \text{for } \mathcal{L} < 0 \text{ (unstable)} \\ 1 & \text{for } \mathcal{L} < 0 \text{ (unstable)} \end{cases} \qquad (9)$$

where $\mathrm{C}_{\,\mathrm{turbulent}}$ = 7.71, u_{*} is the surface friction velocity, $\mathcal{L}$ is the Monin-Obukhov length, and $\mathrm{z_i}$ is the height (set up as $\mathrm{z_i}$ = 1000 m).

The convective term $\Delta\mathrm{WG}_{\,\mathrm{convective}}$ in the sum was added later by Bechtold & Bidlot (2009) to include the gustiness in deep convective situations with strong wind shear, as frontal systems and long-lived organized mesoscale convective systems (which would have not been captured by $\Delta\mathrm{WG}_{\,\mathrm{turbulent}}$). It is calculated as proportional to the non-negative low-level wind shear $\Delta\mathrm{WS}^{+}_{\mathrm{shear}}$:

$$\Delta\mathrm{WG}_{\,\mathrm{convective}} = \mathrm{C}_{\,\mathrm{convective}} \cdot \Delta\mathrm{WS}^{+}_{\mathrm{shear}} \qquad (10)$$

with

$$\Delta\mathrm{WS}^{+}_{\mathrm{shear}} = \max\left(\mathrm{WS}_{\,850} - \mathrm{WS}_{\,950}\right) \qquad (11)$$

where $\mathrm{C}_{\,\mathrm{convective}}$ = 0.6 is a tunable convective "mixing" parameter, and $\mathrm{WS}_{\,850} - \mathrm{WS}_{\,950}$ is the difference between the 850 hPa and the 950 hPa wind speeds, representing the low-level wind shear.

The sum of turbulent $\Delta WG_{turbulent}$ and convective $\Delta WG_{convective}$ terms contribute to the total gustiness. Recalling the physical mechanisms at the origin of the atmospheric turbulence (see Section 3.1), both mechanical and thermal turbulence are included in the presented parametrization, in particular:

- mechanical turbulence is included in $\Delta WG_{turbulent}$ through friction velocity (shear-stress);

- thermal turbulence is included in $\Delta WG_{turbulent}$ through the Monin-Obukhov length, which expresses the ratio between buoyancy and stability of the boundary layer, i.e. the ratio between thermal and mechanical production of turbulent kinetic energy;

- $\Delta WG_{convective}$ includes both mechanical and thermal turbulence of low-level wind shear caused by mesoscale deep convective situations.

4.2 Model datasets

Along this thesis, various types of model datasets are used to investigate surface wind changes and/or are evaluated in comparison to in-situ observations. In particular, three different datasets are considered:

- General Circulation Models (GCMs)
- Regional Climate Models (RCMs)
- Reanalyses

4.2.1 General Circulation Models from CMIP6

Based of physics laws, GCMs are mathematical simulations of the climate system able to represent physical processes and interactions between atmosphere, ocean, cryosphere and land surface (IPCC 2018). By simulating the response of the global climate system to changes in different climatic forcing, GCMs can be employed for understanding climate and forecasting climate change under different scenarios.

In this thesis (Paper II), the Coupled Model Intercomparison Project Phase 6 (CMIP6) historical simulations are used to attribute the anthropogenic causes behind global near-surface WS changes. In CMIP6 historical experiments, the climate system is simulated from 1850 to near-present driven by different historical forcing, as: (i) greenhouse gases (GHGs) concentrations, (ii) land-use changes, (iii) solar and volcanic forcing, (iv) sea surface temperature (SST) and sea ice concentration, and (v) stratospheric aerosols (Eyring et al. (2016). Among the various models participating in the CMIP6 framework, only three models (see Table 1) are considered here as they have at least 10 ensemble members for all the experiments.

Table 1. List of the three CMIP6 models used in this thesis (Paper II).

Model	Institute	Reference
CanESM5	Canadian Centre for Climate Modelling and Analysis	Swart et al. (2019)
CNRM-CM-6-1	Centre National de Recherches Météorologiques	Voldoire et al. (2019)
IPSL-CM6A-LR	Institute Pierre Simon Laplace	Boucher et al. (2018)

4.2.2 Regional Climate Models from Euro-CORDEX

A RCM is a limited-domain climate model which, forced by lateral and ocean conditions from a GCM or an observation-based dataset (reanalysis), simulates atmospheric and land surface processes of the Earth system with regional refinements (AMS 2013). This improved accuracy is enabled, for example, by the more detailed surface characteristics and higher-resolution topography. Because the RCM domain is limited, boundary values are provided by the coarser driving model (GCM or reanalysis). By downscaling global reanalyses or GCMs, large-scale flow is included in the regional simulations, while regional and small-scale circulation features are generated by the RCM. Therefore, RCMs enable more detailed study not only of the mean conditions, but also of extremes (Beniston et al. 2007), by running climate simulations at higher resolution in both time and space (typically at horizontal scales of 10-50 km) than GCMs.

Rather than exhaustively analyzing all possible RCM available across Sweden, only two RCMs are selected and compared with observations (Paper III) to reveal new insights into regional wind gust climate simulations by identifying: (i) the observed features missed by current RCMs; (ii) the advantages of RCM downscaling compared to GCMs; and (iii) the factors in the RCM setup which affect most the model performance in simulating wind gusts (e.g., lateral boundary conditions, gust parametrization, etc.). For this reason, among all the models available in the Coordinated Regional Downscaling Experiment across Europe (Euro-CORDEX, Giorgi et al. 2009), wind gust outputs from two RCMS are analyzed: (i) RCA4 from the Rossby Centre (Strandberg et al. 2014); and (ii) RACMO22E from the Royal Netherlands Meteorological Institute (van Meijgaard et al. 2012). Both models provide data on a horizontal spacing of 0.11° (~12.5 km) and have been run with same boundary conditions: ERA-Interim (hereafter, ERAINT), and two different GCMs - ICHEC-EC-EARTH (hereafter, ICHEC) and MOHC-HadGEM2-ES (hereafter, MOHC) from the fifth phase of the Coupled Model Intercomparison Project (CMIP5; Taylor et al. 2012). To calculate WG, each RCM uses a different gust parametrization. RCA4 estimates WG following Brasseur (2001), while RACMO22E adopts the formulation of Panofsky et al. (1977) and Bechtold & Bidlot (2009) (see Section 4.1).

4.2.3 Reanalyses

Reanalyses provide spatially complete and physically coherent simulated data of various global climate variables by using a forecast model in which information from observations of various types and from multiple sources are assimilated (Dee et al. 2011). Physical coherence is ensured as estimated variables are made to be consistent with the law of physics of the forecast model as well as with the observations; spatially completeness is achieved by using the model equations to extrapolate information from observed variables to unobserved parameters at nearby locations. Historical reanalyses, which span a century or longer, assimilate only near-surface conventional observations as surface pressure and marine winds, which have been available for the entire time period (Slivinski et al. 2019). In modern reanalyses, which generally only extend back to the 1950s (more often to 1979), also upper-air and satellite data are assimilated. Note that all near-surface wind observations over land are excluded because they cannot be usefully interpreted by the data assimilation system (Dee et al. 2011). Instead, terrestrial vertical wind speed profiles from multiple sources (satellites, radio- and aircraft-sondes, etc.) are used as inputs (ECMWF 2020).

This thesis uses two 20th century historical and 6 modern reanalyses (Paper II; see Table 2). In particular, a large focus is given to ERA5 (Paper IV and Paper VI). ERA5 is the latest climate reanalysis produced by ECMWF, which has replaced the highly successful ERAINT (started in 2006). ERA5 benefits from 10 years of developments in model physics and data assimilation (Hersbach et al. 2018). It includes hourly outputs (versus 3-hourly ERAINT outputs), with an increased resolution of 31 km, compared to the 80 km of ERAINT.

Table 2. List of the 6 reanalysis products used in this thesis (Paper II, Paper IV and Paper VI).

Reanalysis	Type	Institute	Reference
NOAA-20C	Historical	National Oceanic and Atmospheric Administration (NOAA)	Slivinski et al. (2019)
ERA-20C	Historical	ECMWF	Poli et al. (2016)
CFSR	Modern	National Centers for Environmental Prediction (NCEP)	Saha et al. (2010)
JRA-55	Modern	Japan Meteorological Agency (JMA)	Kobayashi et al. (2015)
NCEP/DOE-2	Modern	NCEP and National Center for Atmospheric Research (NCAR)	Kanamitsu et al. (2002)
MERRA-2	Modern	NASA Global Modeling and Assimilation Office	Gelaro et al. (2017)
ERA-Interim	Modern	ECMWF	Dee et al. (2011)
ERA5	Modern	ECMWF	Hersbach et al. (2018)

5 Results and discussion

5.1 Global changes in near-surface wind speed

What are the factors that drive the multidecadal changes in global near-surface wind speed?

Before looking at near-surface wind variability across Sweden, the bigger picture of global WS changes is analyzed. Therefore, in Paper II, through the use of reanalyses and GCMs, the global variability in near-surface WS is explored and the possible reasons behind those changes are explored.

First, the trends in global WS during 1980-2010 and 2010-2019 are investigated using eight reanalysis datasets. Multiple reanalyses are used as a reanalysis dataset that stands out in one region may has worse performance in other regions. During 1980-2010 the majority of the reanalysis datasets show significant negative trends over land and positive over ocean (Figure 6). This weakening of Northern Hemisphere (NH) land WS and intensification of Southern Hemisphere (SH) ocean WS are consistent with the findings of previous studies based on in-situ observations (L'Heureux et al. 2013; Zeng et al. 2019). From around 2010 a break in the NH wind stilling and in the SH wind strengthening appears (Figure 7): that is, WS over NH land (SH ocean) underwent increasing (decreasing) trends during 2010-2019, once again recalling the recent reversal of the "terrestrial stilling" (Zeng et al. 2019).

Generally, all the reanalyses agree on observed WS trends. In addition, the spatial distribution of WS suggests an interhemispheric asymmetry of the WS trends over the last decades, with trends over NH opposite to the ones over the SH oceans.

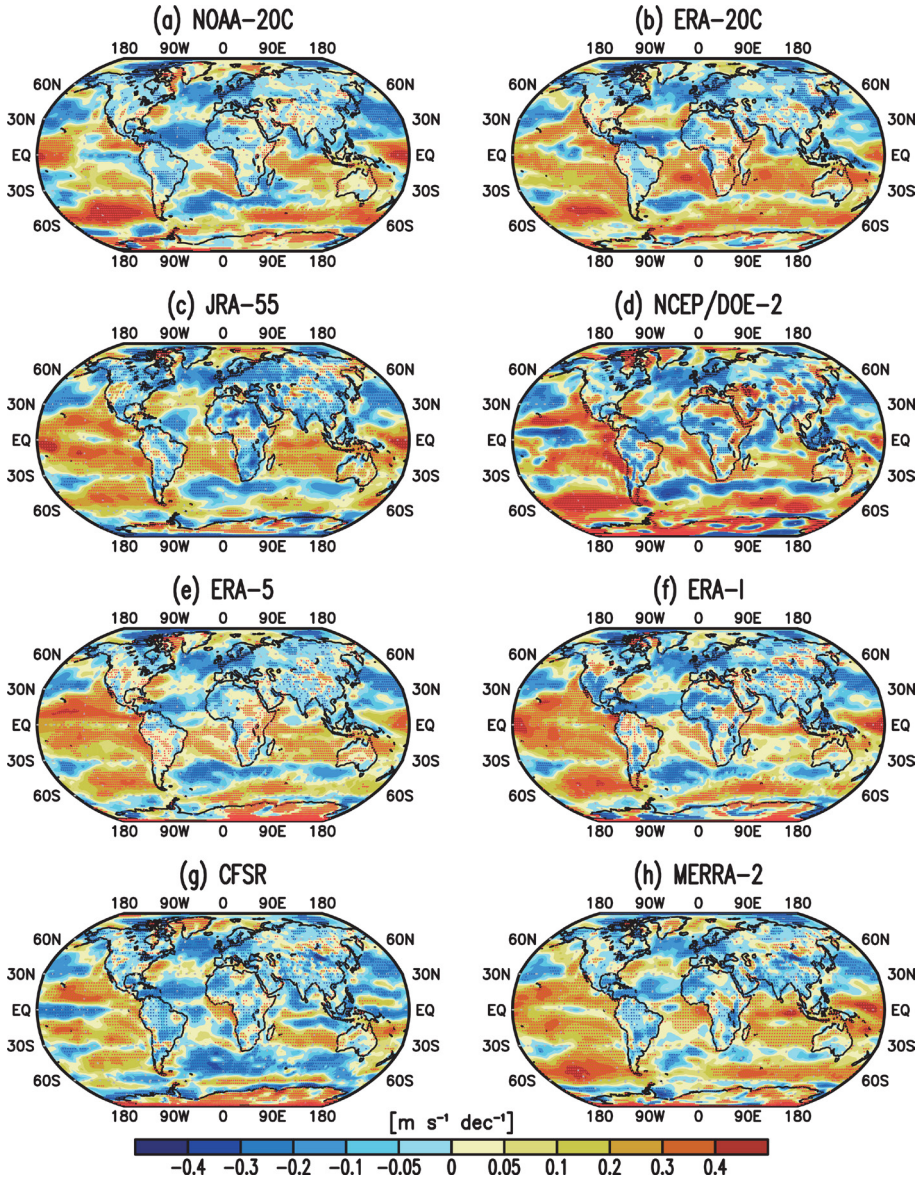

Figure 6. Trends in global near-surface (10 m) WS (unit: m s^{-1} dec^{-1}) during their common period (1980-2010), for (a) NOAA-20C, (b) ERA-20C, (c) JRA-55, (d) NCEP-DOE-2, (e) ERA-5, (f) ERA-I, (g) CFSR, and (h) MERRA-2. The stippling shows statistically significant ($p < 0.1$) grid points (Figure 1 from Paper II).

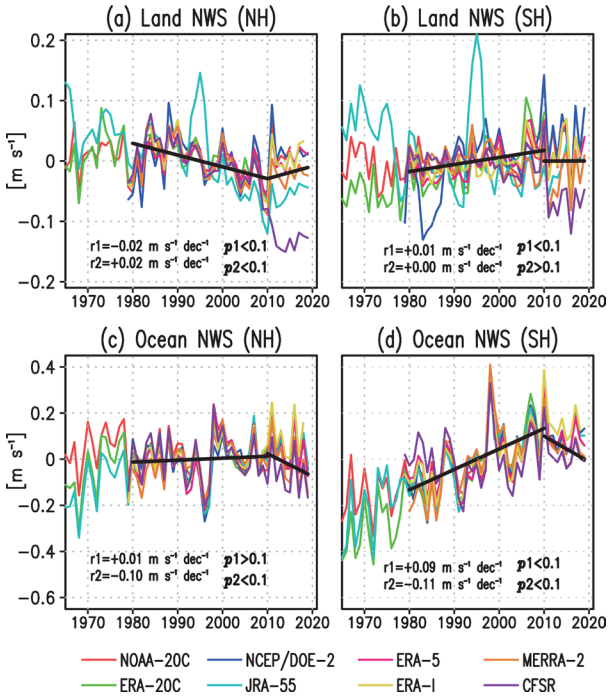

Figure 7. Annual mean WS (unit: m s^{-1}) over (a) the NH land, (b) the SH land, (c) the NH ocean, and (d) the SH ocean, which are expressed as anomalies from the climatology (1980-2010). Color curves indicate the results from eight reanalysis datasets, while black lines denote the linear regressions of averaged WS during 1980-2010 (trend: r1) and 2010-2019 (trend: r2). Significances of the averaged WS trends during the two periods ($p1$ and $p2$) are shown separately in the panels (Figure 2 from Paper II).

To understand the reasons behind these global trend patterns, the impacts of anthropogenic forcing on global WS is analyzed. The comparison with trends from CMIP6 model simulations demonstrates that anthropogenic forcing (e.g. emissions of GHGs and aerosols) was a major force for global WS changes during 1980-2010. In particular, positive WS trends over the SH ocean could be mainly attributed to the GHG forcing, whereas the aerosol forcing tend to force negative WS trends over both hemispheres (Figure 8).

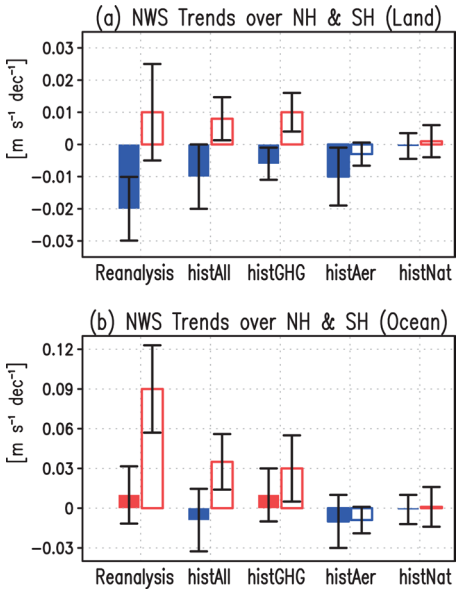

Figure 8. Annual WS trends (bar, unit: m s^{-1} dec^{-1}) over land and ocean during 1980-2010 and their uncertainties (error bar) for the eight reanalysis datasets and CMIP6 model simulations. Filled (open) rectangles indicate the trends averaged over the NH (SH). The uncertainty spread is determined by one standardized deviation of the WS trends (Figure 7 from Paper II).

GHG-induced warming impacts global WS patterns by enhancing tropical convection and thus strengthening the Hadley cell over the SH during 1980-2010 (Figure 9). In fact, land surfaces warm faster than the ocean ones. As SH is dominated by oceans, while NH is mainly covered by land areas, more warming is expected in the NH than the SH in a changing climate (Kang et al. 2015). The Hadley cell is more likely to strengthen in the colder hemisphere, with an opposite response in the warmer one (Hack et al. 1989; McGee et al. 2014). A strengthening of the SH Hadley cell intensifies SH trade winds and sub-Antarctic westerly winds, and this leads to the overall increase in SH WS.

If changes in SH Hadley cell can reasonably account for the strengthening of the SH WS during 1980-2010, they failed to explain the "wind stilling" feature over land in the NH. Instead, increased surface roughness over land during the last decades (e.g. human land-use activities, urbanization, greening) could partly account of the trends detected here, but are not sufficient to explain all the magnitude of decline. Additional factors can thus affect WS changes over NH land. For example, previous studies have indicated that the weakening of NH atmospheric circulation could be influenced by accelerating Arctic warming through losses of Arctic sea ice (Coumou et al. 2015; Cohen et al. 2020). In fact, sea ice losses can induce remarkable surface warming over the Arctic regions by changing the surface albedo. Compared to lower latitudes, the warmings of air temperature in the Arctic and surroundings are thus faster. This reduces the equator-to-pole temperature gradient, which explains the slowdown of thermally driven zonal winds over the NH middle latitudes.

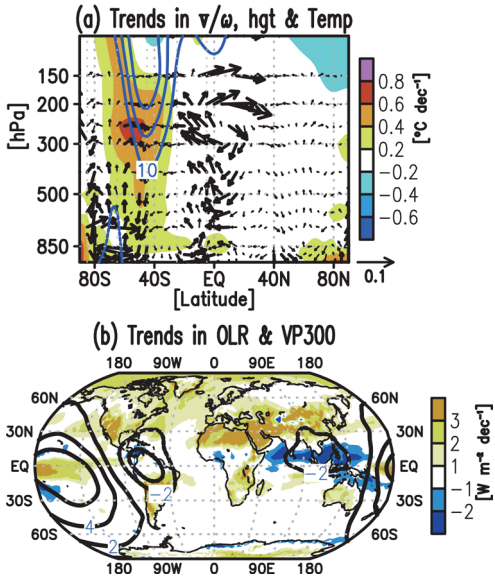

Figure 9. (a) Zonal averages of trends in annual meridional and vertical (multiplied by -100) winds (vector, unit: m s^{-1} dec^{-1}), geopotential heights (contour, unit: m dec^{-1}), and air temperatures (shading, unit: °C dec^{-1}) during 1980-2010. (b) Similar to (a) except for the spatial distributions of trends in annual OLR (shading, unit: W m^{-2} dec^{-1}) and 300-hPa velocity potential (contour, unit: 10^4 dec^{-1}). The trends in winds and OLR are obtained from the ERA5 and NOAA interpolated-OLR datasets, respectively (Figure 8 from Paper II).

But what can explain the reversed trends in global WS observed since 2010? Figure 9 clearly shows that the enhanced convection over the West Pacific and tropical Atlantic is followed by a strong suppressed convection over the East Pacific. This spatial distribution recalls the Pacific Decadal Oscillation (PDO) variability. In fact, the phase changes in the PDO follow well the recent reversal of global WS. More specifically, during 1980-2010, PDO underwent a positive-to-negative phase change that induced warming SST trends in the West Pacific and cooling SST trends in the Central and East Pacific (Figure 10). This resulted in an intensified equatorial Pacific zonal SST gradient and enhanced convection over the West Pacific: Hadley cell intensifies and WS strengthens over the SH. Instead, the negative-to-positive phase change in PDO during 2010-2019 brings warming SST trends in the East Pacific and cooling SST trends in the West Pacific, reducing the equatorial Pacific zonal SST gradient and suppressing the West Pacific convection. As a result, the SH Hadley cell becomes weaker, and this could cause the beak in SH WS increase. Moreover, SST increased during 1980-2010 in the North Atlantic and North Pacific, decreasing the meridional temperature gradient, which weakens westerly winds over the NH. Opposite, during 2010-2019, cooling SST trends trigger in the same way the intensification of the NH westerly winds (e.g., Coumou et al. 2015). That is, since 2010, the phase changes of PDO could have played a more dominant role in modulating the WS trends than the GHG forcing, which reasonably explains the reversed trends in global WS.

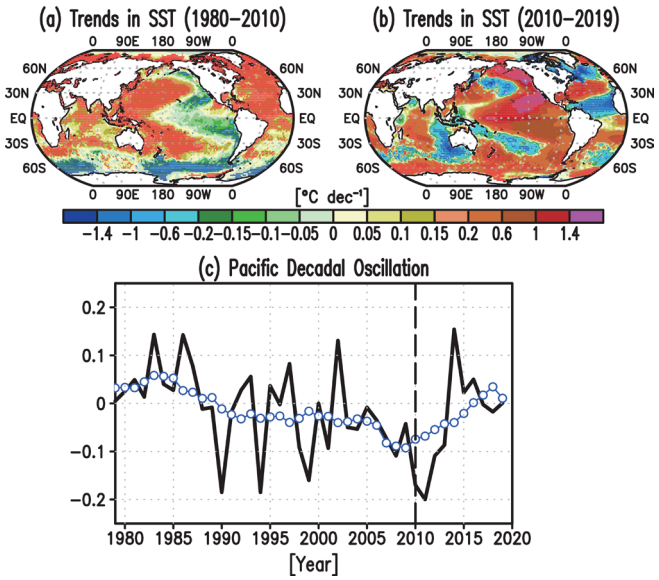

Figure 10. Trends in annual SST (unit: °C dec^{-1}) during (a) 1980-2010 and (b) 2010-2019, obtained from the ERA5 reanalysis. (b) Index of the annual mean PDO (black line), whereas the blue curve indicates the 9-year running mean. The stippling shows statistically significant ($p < 0.1$) grid points (Figure 11 from Paper II).

To summarize, terrestrial WS over the NH experienced significant decreasing trends during 1980-2010, while SH ocean winds were characterized by significant increasing trends. The increased GHG plays an important role in triggering those trends. In particular, the significant WS increase over the SH is primarily attributed to the intensified SH Hadley cell related to GHG-induced forcing, while the NH land slowdown is likely caused by increase in surface roughness (e.g. greening) together with the accelerating Arctic warming. However, since 2010, global WS shifted in their sign: such reversal is likely associated with the negative-to-positive phase changes in the PDO, which lead to the weakening of the Hadley cell over the SH and to strengthened westerly winds over the NH. A schematic summary of those described possible causes behind the global WS changes is shown in Figure 11.

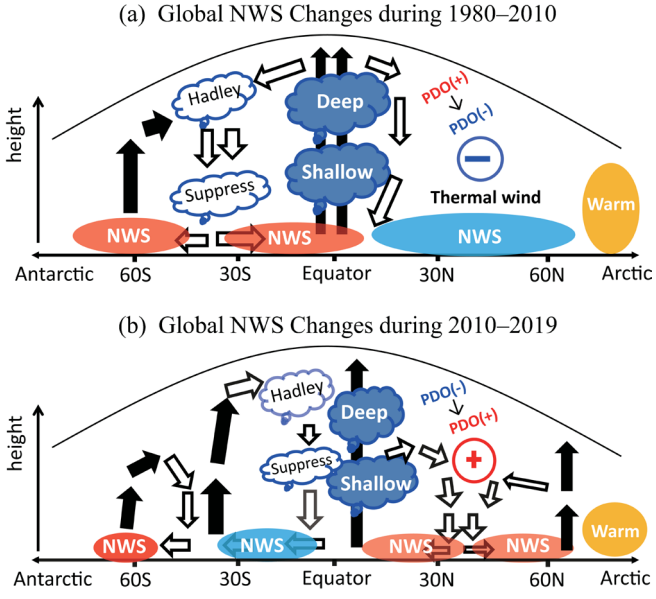

Figure 11. Schematic diagrams of possible causes of global WS changes during (a) 1980-2010 and (b) 2010-2019 (Figure 13 from Paper II).

5.2 Climatology of observed surface winds across Sweden

What is the observed climatology of near-surface winds across Sweden?

Wind climatology is strongly dependent on terrain characteristics of the region (Jimenéz & Dudhia 2012). In fact, topographic features influence the surface energy balance, and, especially over mountainous terrain, the atmospheric boundary layer (ABL) is shaped by thermally- and dynamically-forced earth-atmosphere exchange processes through turbulent transport (Rotach et al. 2016; Helbig et al. 2017). The resulting inhomogeneous ABL drives mesoscale and even sub-mesoscale flows (e.g., slope and valley winds), which strongly affect the regional wind characteristics. When plotting mean WS or WG conditions for each station versus the station distance to the sea and its elevation (Figure 12), measuring stations across Sweden can be classified into three groups, where winds are influenced by similar physical processes driven by related terrain characteristics:

- Coast stations, where wind conditions are dominated by regional and local circulations due to differences between sea and land (e.g., sea breezes, turbulence due to step-like change in surface roughness; Gustavsson et al. 1995; Borne et al. 1998);

- Inland stations, strongly influenced by land surface processes and earth-atmosphere interaction through turbulent transport, driven for example by friction and heat exchange (Rotach et al. 2016);

- Mountain stations, where the complex topography favors the development of local wind systems which are often suppressed by stronger larger-scale winds in the free troposphere (Rotach et al. 2016; Serafin et al. 2018).

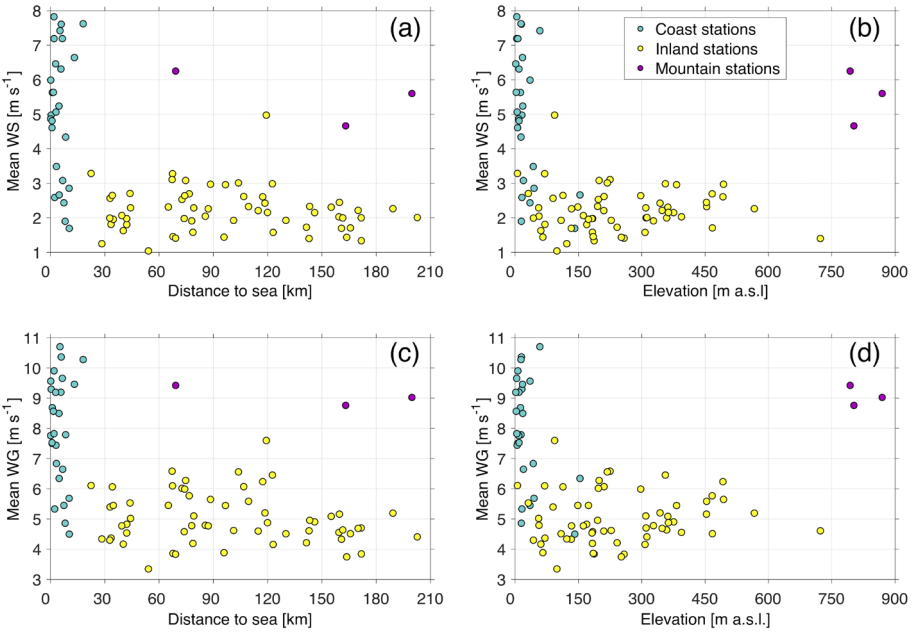

Figure 12. Scatterplot of mean WS (top row) and mean WG (bottom row) of the 90 weather stations across Sweden for 2013-2017 plotted against the station distance to the sea (left) and its elevation (right). Scatter-points are clustered into three groups: (1) coast stations (blue-green), (2) inland stations (yellow), and (3) mountain stations (violet) (Figure 2 from Paper IV).

The spatial and temporal patterns of observed near-surface WS across Sweden for 1999-2000 were already presented by Achberger et al. (2006). Achberger et al. (2006) showed that the annual mean WS across Sweden varies between 2 and 5 m s^{-1}, with higher values at exposed mountainous sites and on islands off the coast. WS decreases rapidly when moving inland from the coast because of the sea-land step-like change in surface roughness. The amplitude of the WS seasonal cycle is strongest at coastal stations and at mountainous locations. It peaks in winter at all coastal and mountainous stations. In contrast, inland regions show a less pronounced seasonal cycle, with a peak between late spring and early summer and weakest mean winds in winter.

Following Achberger et al. (2006), the observed DPWG climatology across Sweden is now investigated in Paper III. Annually, coastal stations generally display higher mean DPWG (greater than 10 m s^{-1}) than the inland stations (~8 m s^{-1}), except for few stations located at high elevations in the Scandes range (~12 m s^{-1}). Seasonally (Figure 13), the observed seasonal cycle of coastal stations shows the strongest winds in winter and the weakest in summer. This seasonality is different for inland stations, where only small differences are detected: slightly higher mean DPWG values are recorded during warmer months (May-June) compared to cooler seasons (winter and autumn). The observed seasonal cycle of DPWG in mountain stations has a strong seasonal-dependent signal similar to the one of coastal stations, with the maximum and minimum values during the cold and warm months, respectively.

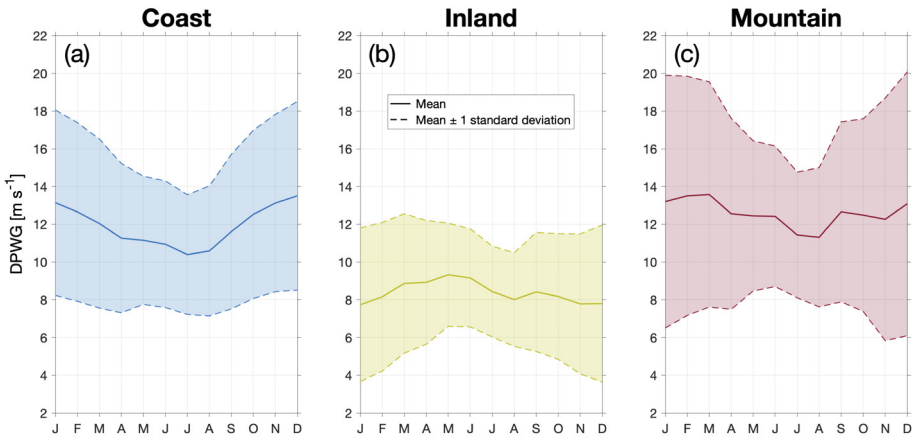

Figure 13. Mean seasonal cycle of DPWG for stations in coastal (left), inland (middle), and mountain (right) regions averaged for 1996-2017. The seasonal cycle is displayed as its mean value (solid line) and the standard deviation (colored area bounded by the dashed line (Figure 5 from Paper III).

Overall, the regional DPWG climate agrees with the one observed for WS in Achberger et al. (2006). Areas (coastal and high elevation stations) with stronger mean winds are also the ones with stronger gustiness. Similar to WS, higher DPWG is recorded during cooler months (e.g., winter) in both coastal and mountain regions, while for inland stations the seasonal cycle of both WS and WG is weak and peaks in late spring or early summer.

5.3 Can we realistically model wind gustiness?

5.3.1 Wind gust in RCMs

Do RCMs have proper skills in simulating DPWG across Sweden?

The performance of current RCMs in simulating DPWG is evaluated in Paper III by using the created homogenized DPWG dataset. Firstly, we investigate if the downscaling of RCMs adds value to DPWG simulations compared to GCMs. In Figure 14, mean DPWG values at each station are plotted as a function of the station's distance to the sea or its elevation for the ERAINT (driving model), RCA4-ERAINT, and RACMO22E-ERAINT datasets. The observed high mean wind conditions at the coastal stations are captured by both ERAINT and RCMs, which include the land-sea contrast and the impact of large-scale circulation. However, when looking at inland stations, ERAINT does not show distinct differences between high-elevation stations and other inland stations, even though both observations and RCMs show greater winds at higher elevation stations. Such differences can be discerned only when topographic features are included. Unfortunately, the too coarse spatial resolution of the driving models (e.g., ERAINT, ~80 km) cannot resolve the complex terrain features responsible for the gustiness and modified flow (Rotach et al. 2016). In contrast, RCMs with their greater horizontal resolution are able to capture the differences between the three observed DPWG regions. RCM simulations, with their higher horizontal resolution, are needed if the features most relevant for explaining the DPWG climatology across Sweden should be included. The use of RCM downscaling for DPWG studies is thus justified, as considered by Kjellström et al. (2005), Rockel & Woth (2007), Nikulin et al. (2010), and Strandberg et al. (2014).

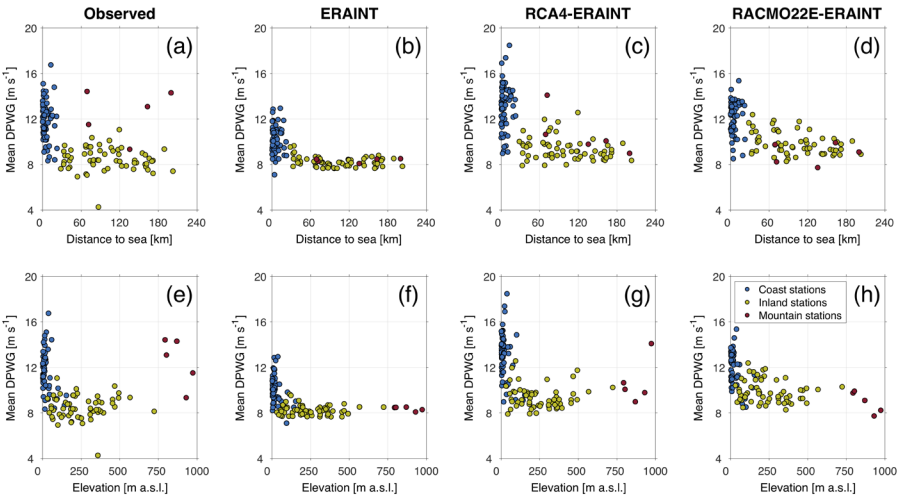

Figure 14. Scatterplot of the 1996-2005 mean of DPWG for the 127 stations across Scandinavia plotted against station distance to the sea (top row) and elevation (bottom row) calculated using (from right to left) the observed, ERAINT, RCA4-ERAINT, and RACMO22E series. Scatter-points are filled according to their region: (i) coast (sky-blue), (ii)inland (olive), and (iii) mountain (brown) (Figure 7 from Paper III).

The use of a consistent set of boundary conditions for both RCMs provides the opportunity to study the role of RCM configuration in the simulated climatology under the same large-scale forcing. Figure 15 shows the spatial distribution of mean DPWG for both RCA4 and RACMO22E driven by three boundary conditions. The spatial patterns of DPWG do not vary much when the same RCM is integrated with different boundary conditions. Instead, the spatial pattern of mean DPWG largely differs between the two RCMs regardless of the boundary conditions (e.g., RCA4 shows a greater west-east or north-south contrast in DPWG compared to RACMO22E). Therefore, when looking at climate averages, the performances of RCMs in simulating DPWG are more sensitive to the dynamics and the physics (e.g., parametrization) of the model than the adopted boundary conditions. Instead, the role of boundary forcing becomes more relevant than the role of the RCM when looking at climate variability and changes (Déqué et al. 2007).

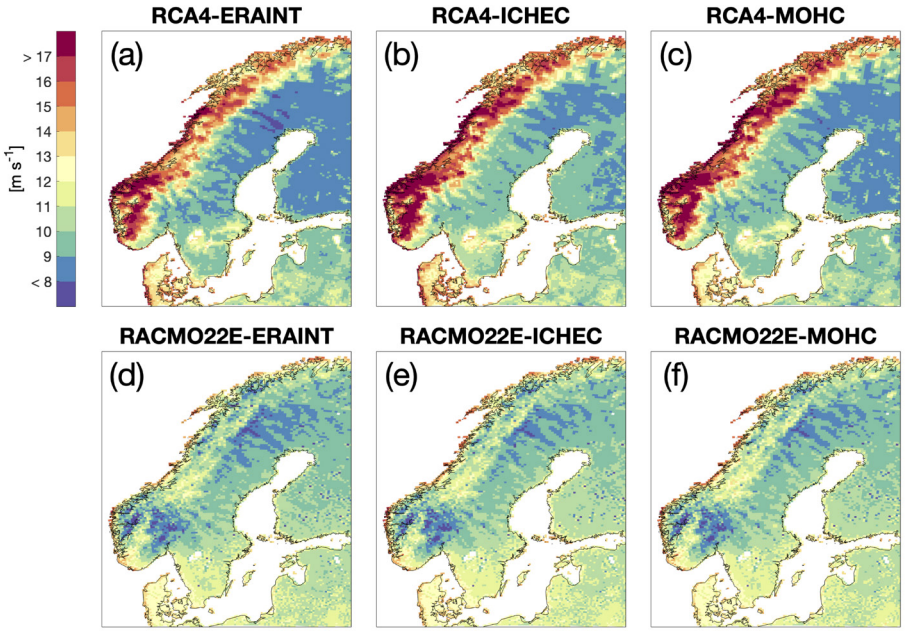

Figure 15. Spatial distribution of the annual 1996-2005 mean DPWG for the RCA4 (top row) and RACMO22E (bottom row) datasets with the ERAINT (left), ICHEC (middle), and MOHC (right) driving models (Figure 9 from Paper III).

When looking at the simulated seasonal cycle (Figure 16), once again both the selected RCMs perform well in reproducing the observed DPWG across coastal regions. In inland areas, they still closely resemble the climate statistics, but discrepancies become more noticeable (e.g., strong RCA4 seasonality vs. weak observed seasonality). Across mountain regions, all RCMs struggle to simulate the observed DPWG features, although the mismatch in RACMO22E is mostly caused by a negative bias.

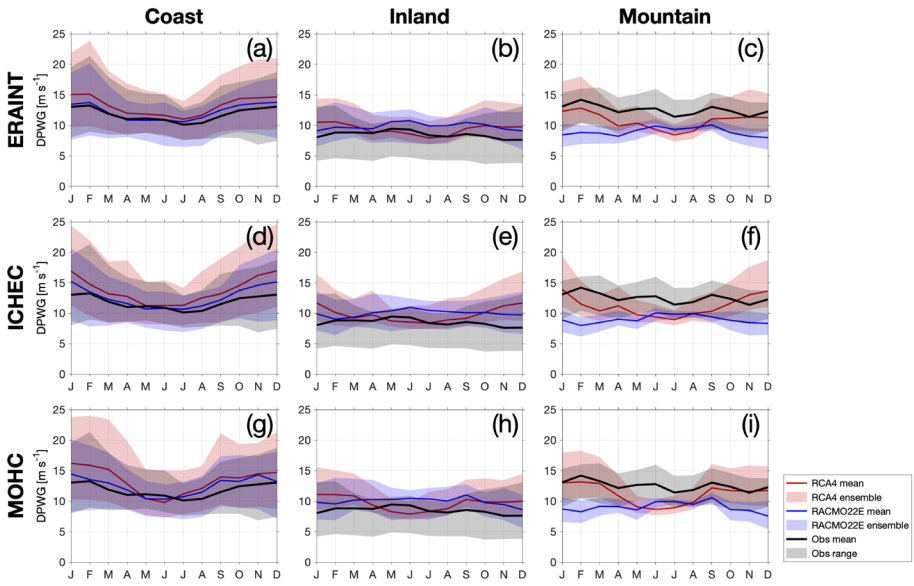

Figure 16. Mean seasonal cycle of DPWG series calculated using observations (black), RCA4 (red), and RACMO22E (blue) with different driving models (ERAINT, top row; ICHEC, middle row; MOHC, bottom row) in coastal (left), inland (middle), and mountain (right) regions for 1996-2005. The seasonal cycle is displayed as the mean (solid line) and the ensemble (colored area) of the seasonal variability for different series in the same dataset (Figure 10 from Paper III).

To summarize, the two selected RCMs are able to model DPWG conditions along the coastline, but show poor skills in simulating inland and mountain wind climate, where surface forcing and sub-grid scale parametrizations play a key role (Kunz et al. 2010). This calls for an even higher resolution, where the downscaling can capture the complex topographic influences, and/or better represent relevant physical processes. Based on these requirements, a promising framework for improving DPWG simulations at regional to local scales can be provided by RCMs using convection-permitting models (CPMs), with a horizontal grid spacing of ~4 km (Prein et al. 2015; Kendom et al. 2017). CPMs have the advantage of explicitly resolving deep convection (e.g., frontal situations and midlatitude summer convective systems; Bechtold & Bidlot 2009; Punkka & Bister 2015), avoiding error-prone convection parametrizations, and better resolving topography and surface forcing in regions with strong spatial heterogeneities (e.g., mountain areas).

5.3.2 Wind gust in ERA5

Does ERA5 have proper skills in simulating WG climate across Sweden?

In Paper IV, the ability of the new ERA5 product to realistically reproduce hourly WG (and WS) across Sweden is tested. In particular, it is evaluated if there are noticeable improvements from its predecessor ERAINT. Statistics for WG (Figure 17) show the best agreement with observations for ERA5. In particular, the mean Pearson's correlation coefficient is higher for ERA5 across all regions, and the mean Root Mean Squared Error (RMSE) and mean bias is smaller compared to ERAINT. ERA5 best agrees with observed WG in coastal areas, where correlation is the highest among all the three regions, while both mean RMSE and bias are the lowest. For inland stations, the mismatch of ERA5 compared to the observed WG is greater, with lower mean correlation and increasing mean RMSE and bias. Especially for mountainous regions, ERA5 struggles to simulate the observed wind characteristics, showing a mean bias larger than 2 m s^{-1} for all the temporal scales considered.

To summarize, ERA5 shows better performance than its predecessor ERAINT in representing WG (and also WS) across Sweden, most likely due to higher resolution (i.e., from 80 to 31 km), the improvements made in the representation of the model processes (better model physics), more data assimilated, and its more advanced assimilation method. However, evident discrepancies are still found across inland and mountain regions.

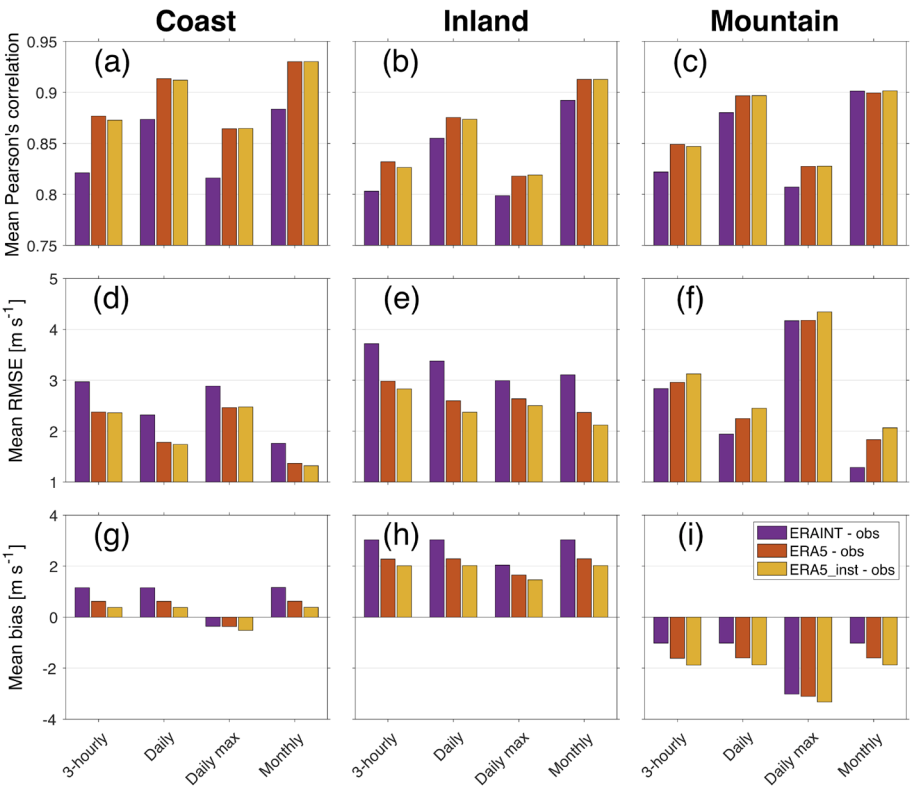

Figure 17. Summary statistics for comparison between observed WG and reanalyzed WG from ERAINT (violet), ERA5 (orange), and ERA5_inst (yellow) at different temporal scales for 2013-2017. For each region it is shown: (1) mean Pearson's correlation (top row), (2) mean RMSE (middle row), and (3) mean bias (bottom row) (Figure 7 from Paper IV).

5.3.3 Towards an improved gust parametrization

Can ERA5 gust parametrization be improved?

Given the discrepancy between ERA5 and observed WS, can a better gust parametrization improve the ERA5 performance in simulating gustiness? For this reason, a close look at the ERA5 gust parametrization is done in Paper IV to test if the parametrization used can realistically represent the physical processes behind the origin of gusts across Sweden.

Figure 18 decomposes the contribution of the different WG parametrization terms of Eq. (4) to the total mean seasonal cycle for the different regions during 2013-2017. In the contribution, $WS_{instantaneous}$ is replaced by the observed WS so that the parametrized WG does not suffer from biases or errors due to the modelled WS and the contribution of each gustiness term ($\Delta WG_{turbulent}$ and $\Delta WG_{convective}$) can be addressed. For the coast stations, the mean seasonal cycle of the parametrized WG, driven by the major contribution of WS, matches the observed cycle well, even if it is slightly underestimated. Across inland areas, although observed and parametrized WG closely agree during winter months, differences are found during the rest of the year. The observed WG shows a weak seasonal variability that peaks during March-June, whereas the parametrized WG does not change much during the year on average. For the mountain stations, the parametrized seasonal cycle (where WS contributes most) resembles the observed one, even thought is constantly underestimated up to 2 m s^{-1} in each month. Notice how the $\Delta WG_{convective}$ contribution in all the three regions does not follow the seasonality of occurrence of deep-convective situations and mesoscale convective systems at the origin of convective gusts in a country like Sweden. In fact, their frequency of occurrence is much higher during the warm months (April-September) than the cold months (October-March) across Finland (Jeong et al. 2011; Punkka & Bister 2015), and this does not agree with the seasonal cycle of $\Delta WG_{convective}$ shown in Figure 18.

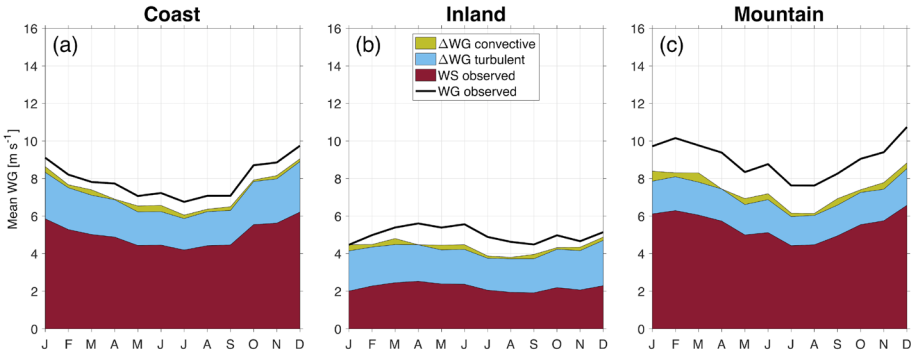

Figure 18. Contribution of the different WG parametrization terms to the mean seasonal cycle across different regions for 2013-2017. In particular, in dark red the contribution of the observed WS is represented, in light blue the one of the calculated $\Delta WG_{turbulent}$, and in yellow-green the added input of $\Delta WG_{convective}$. In black the mean seasonal cycle from the observed WS is shown (Figure 10 from Paper IV).

The identified discrepancy in the mean seasonal cycle between the observed and simulated WG suggests that the gust parametrization could be improved across Sweden. For this reason, the WG is thus adjusted by tuning for each station both the $C_{turbulent}$ of the $\Delta WG_{turbulent}$ term and $C_{convective}$ of $\Delta WG_{convective}$. In particular, using multi-regression, for each station and using all time step available, the function in Eq. (12) is fitted following the parametrized gust formulation of Eq. (7):

$$Y = C_{turbulent} \cdot \Delta WG_{friction+stability} + C_{convective} \cdot \Delta WS^{+}_{shear} + C_{unexplained} \quad (12)$$

with

$$Y = WG_{obs} - WS_{obs} \quad (13)$$

where $C_{unexplained}$ represents what the turbulent and convective contributions cannot explain in the difference between observed WG and WS. The different coefficients ($C_{turbulent}$, $C_{convective}$ and $C_{unexplained}$) of Eq. (9) are calculated by different tuning procedures in order to evaluate the importance of each term in the parametrization:

- *Tuning procedure 1*: With the fixed $C_{convective} = 0.6$, the coefficients $C_{turbulent}$ and $C_{unexplained}$ are calculated for each station.

- *Tuning procedure 2*: The coefficients $C_{convective}$ and $C_{unexplained}$ are calculated keeping $C_{turbulent}$ fixed to 7.71.

- *Tuning procedure 3*: $C_{turbulent}$, $C_{convective}$ and $C_{unexplained}$ are all calculated by multi-regression.

When plotting the different coefficients against station elevation (Figure 19), the distribution of $C_{turbulent}$ shows an elevation-dependency that is fitted by linear regression with the $C_{turbulent}$ function having the form:

$$C_{turbulent}(h) = A \cdot h + B \quad (14)$$

where h is the station elevation, A and B are the coefficients of the best-fit curve. $C_{convective}$ does not display any elevation-dependency in its distribution, but its average value is much lower than the 0.6 suggested by Bechtold & Bidlot (2009).

Following what shown so far, Paper IV aims at improve the parametrization of WG by:

- implementing an elevation-dependency in the $\Delta WG_{turbulent}$ contribution through a $C_{turbulent}$ function able to take elevation differences among different regions into account;

- tuning the $\Delta WG_{convective}$ term through the adjustment of the $C_{convective}$ coefficient according to the observed WG climate across Sweden.

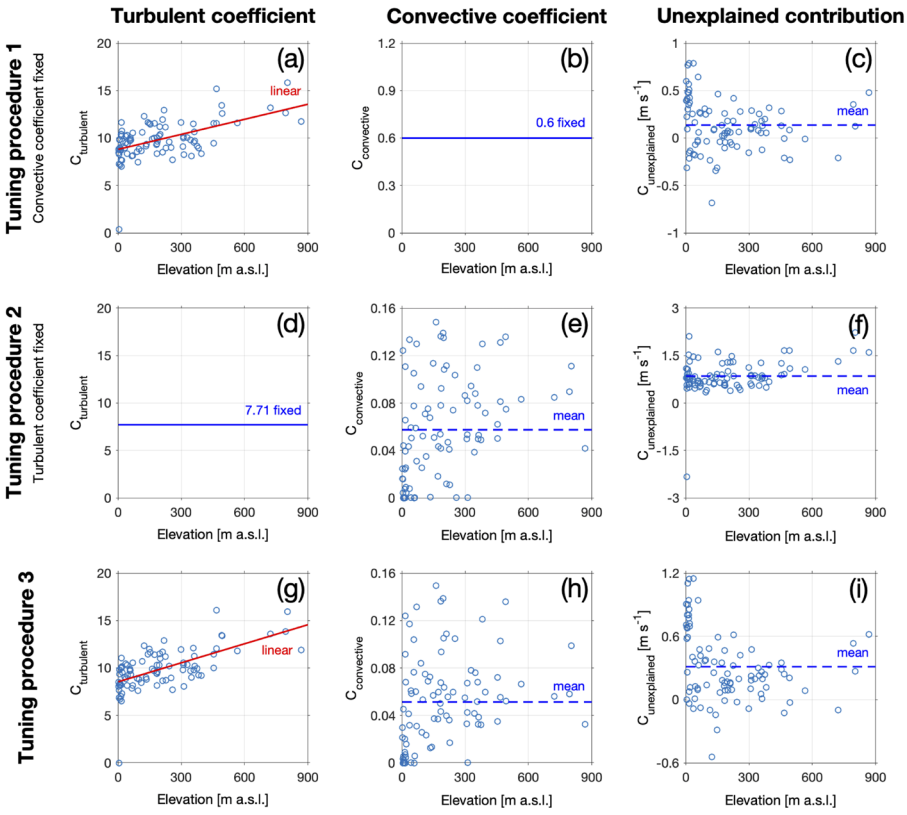

Figure 19. Distribution of the C $_{turbulent}$ (left column), C $_{convective}$ (middle column) and C $_{unexplained}$ (right column) coefficients versus the measuring station's elevation in the *tuning procedure* 1 (top row), *tuning procedure* 2 (middle row), and *tuning procedure* 3 (bottom row). In red the linear regression which fit best to the distribution is shown. The dashed blue line is the mean value of the distribution. If a coefficient was fixed in the tuning procedure, its value is displayed as blue line (Figure 11 from Paper IV).

In comparing the different parametrizations (Figure 20), mean Pearson's correlations are higher for both *convection tuned* and *turbulence function + convection tuned* parametrizations compared to the standard parametrization: when the convective gust contribution is tuned, it is improved how the WG variability is parametrized. But for the *convection tuned* WG, there are no improvements in both mean RMSE and bias compared to the *standard* parametrization: the C $_{convective}$ tuning cannot improve the evident negative bias. This bias can be reduced, especially across mountain regions, when an elevation-dependency is implemented in the turbulent contribution.

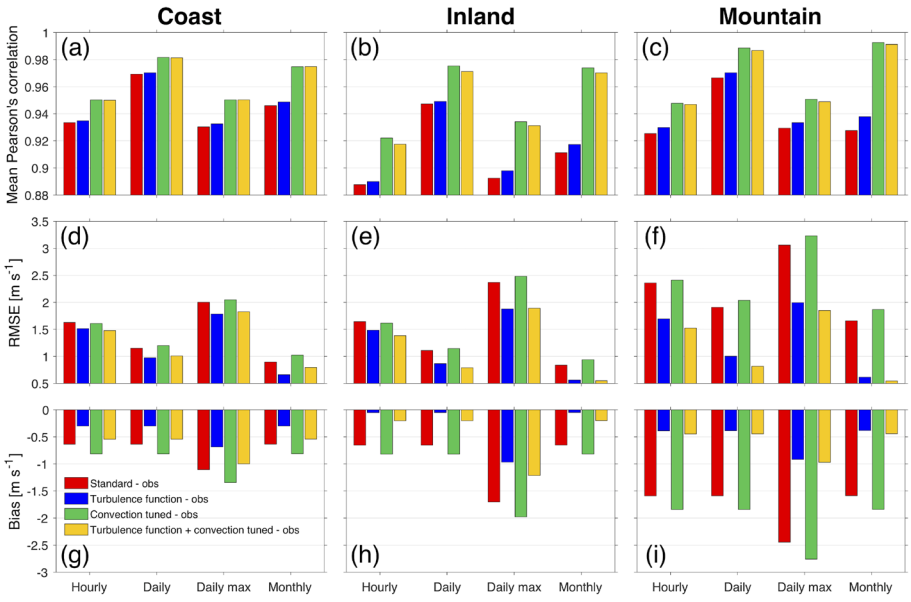

Figure 20. Summary statistics for comparison between observed WG and WG from *standard* (red), *turbulence function* (blue), *convection tuned* (green), and *turbulence function + convection tuned* (yellow) parametrizations during 2013-2017. In particular, for each region (coast, inland, mountain) (1) mean Pearson's correlation (top row), (2) mean RMSE (middle row), and (3) mean bias (bottom row) are shown (Figure 13 from Paper IV).

To summarize, a better performance in the simulation of WG can be achieved in the new *turbulent function + convection tuned* parametrization, when both a turbulent function is implemented and the convective gust term is tuned. In particular, results show that:

- by implementing an elevation-dependency in the turbulent contribution, the negative bias displayed by the standard parametrization can be reduced;
- by tuning the convective term, higher correlation with the observed WS is reached.

The physical explanation for the need of an elevation-dependency in the turbulent contribution lies in the formulation of Panofsky et al. (1977) to express turbulent gusts, which requires a horizontally homogeneous surface. In fact, all the data analyzed by Panofsky et al. (1977) were obtained over those flat surfaces where the Monin-Obukhov similarity hypothesis is valid (Arya 2001). In line with this limitation, Panofsky et al. (1977) clearly stated that "it is quite possible that mesoscale terrain features can influence the scale of horizontal velocity components". Over the land grid of a climate model, such as the one used for ERA5, the condition of homogeneity cannot be guaranteed. Any atmospheric model, with its inherent spatial discretization, has to smooth the surface physical properties such as orography (Jiménez & Dudhia 2012). The approximation of smoother topography is less accurate especially over mountainous areas, where the heterogeneity driven by valleys and mountains becomes relevant. For example, unresolved topographic features can introduce biases in wind simulations across complex terrain regions (Jiménez & Dudhia 2012). The elevation dependency of the turbulent gusts found here points to the need of including unresolved topography in the WG parametrization, for example through the use of the elevation-dependent $C_{turbulent}$ function.

Results also show that the gust forecasting ability is improved by calibrating the convective contribution with observational data. Statistically, such tuning procedure works, but it cannot be considered adequate: it should be explored a better formulation of $\Delta WG_{convective}$ which expresses more realistically the relevant physical processes at the origin of convective gustiness across Sweden. This need is supported by the fact that $\Delta WG_{convective}$ seasonality is not in line with the seasonal occurrence of deep-convection situations and mesoscale convective systems at the origin of gustiness (Figure 18). Bechtold & Bidlot (2009) have related the maximum gust from deep-convection to low-level wind shear as a sheared environment is needed to increase the potential for a mesoscale convective system to produce severe surface winds through a stronger and more organized structure (Cohen et al. 2007). For a region like Scandinavia, convective gusts may need to be calculated in relation to a different definition of low-level wind shear (e.g. a deeper layer shear; Cohen et al. 2017) or by different proxies of maximum gustiness (Johns & Doswell 1992).

5.4 Near-surface mean and gust wind speed variability across Sweden

How did mean and gust wind speed change across Sweden?

In Paper V and VI the long-term variability of mean and gust wind speed across Sweden is investigated using the homogenized wind series. In particular, Paper V investigates trends of homogenized series of monthly mean wind observations from 24 weather stations covering the 1956-2013 time period, with a focus on 1979-2008 (with an addition of 9 stations) for comparison with previous studies. The dataset displays a significant downward trend for 1956-2013 (-0.06 m s^{-1} dec^{-1}) and an even larger decreasing trend for 1979-2008 (-0.14 m s^{-1} dec^{-1}) (Table 3). The decreasing trend is more pronounced at coastal stations in southern Sweden (Figure 21). Such slowdown magnitude is in line with the one reported for nearby countries (e.g., Netherland, -0.09 m s^{-1} dec^{-1}; Cusack et al. 2013) or regions of close latitude range (Canada, -0.05 m s^{-1} dec^{-1}; Wan et al. 2010) for a similar time period. However, differences have been observed seasonally, with significant decreasing values in spring, summer, and autumn; while the winter slowdown is less pronounced (Table 3 and Figure 21). Whereas the wind decreasing for Sweden is mainly observed in summer and less evident in winter, the summer in the Iberian Peninsula (i.e., Spain and Portugal) is the season with the highest rate of stations showing increasing WS (Azorin-Molina et al. 2014).

Table 3. Annual and seasonal wind speed trends (m s^{-1} dec^{-1}) averaged over all the stations for 1956-2013 (24 stations) and 1979-2008 (33 stations). Statistically significant trends are shown in boldface for $p < 0.05$ and in italic for $p < 0.10$ (Table 1 from Paper V).

Period	1956-2013	1979-2008
Annual	**-0.06**	**-0.14**
Winter (DJF)	-0.04	-0.01
Spring (MAM)	**-0.06**	**-0.15**
Summer (JJA)	**-0.10**	**-0.11**
Autumn (SON)	**-0.07**	**-0.26**

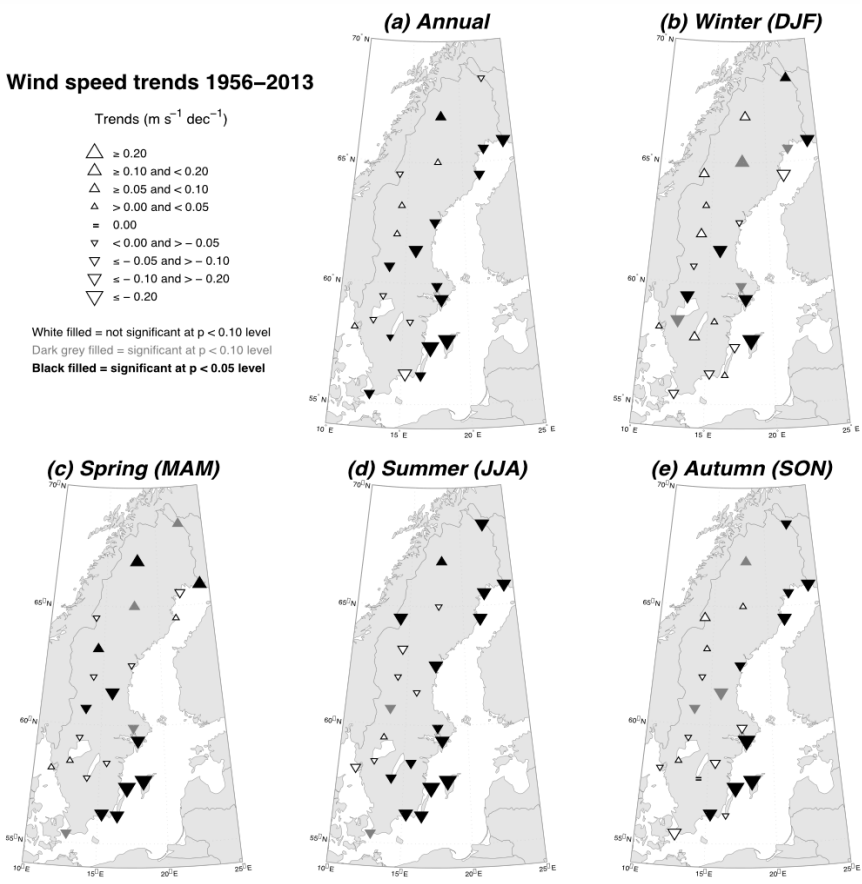

Figure 21. Annual and seasonal spatial distribution of the sign and magnitude of trends (m s^{-1} dec^{-1}), and statistical significance (black filled triangles are significant at $p < 0.05$, dark gray triangles are significant at $p < 0.10$, and unfilled triangles are not significant at $p > 0.10$) of wind speed trends for the homogenized series of the 24 stations for 1956-2013 (Figure 5 from Paper V).

The seasonal differences in the magnitude and sign of WS trends between northern and southern Europe can be explained by the NAO circulation. NAO describes the relative changes in pressure between the Icelandic low-pressure region and the relatively high-pressure centered over the Azores islands (NOAA 2012). To quantify the strength of this circulation pattern and its interannual variability, the NAO index is defined as the normalized sea-level pressure difference between Gibraltar and southwestern Iceland (e.g., Reykjavik) (Jones et al. 1997).

Results here show strong and significant (at $p < 0.05$) correlation between NAO index and WS variability (Figure 22). In fact, the NAO drives the changes in the intensity and location of the North Atlantic jet stream, thus influencing the movement of regions of low pressure and their associated midlatitude cyclones. It is particularly important in winter, when it exerts a strong control on the climate of the northern hemisphere (Wallace & Gutzler 1981; Hurrel 1995), and it has been proven to be one of the most influential atmospheric teleconnections for climate variability in Sweden (Hurrell & van Loon 1997; Chen & Hellström 1999; Linderholm et al. 2011). In particular, during the positive NAO phase (positive NAO index, i.e. stronger than usual difference in pressure between the two regions), westerly winds with their warm air dominate, while the position of the jet streams enables more and stronger storms to travel across the Atlantic (Met Office 2018). Thus, mild, stormy and wet winters result in northern Europe, while southern Europe experiences cold and dry winter conditions. On the opposite, during negative NAO phase (negative NAO index, i.e. weaker than usual difference in pressure), easterly and north-easterly winds are stronger, bringing cold air to northern Europe, which experience cold, calm and dry winters. Weaker and less frequent storms characterize northern European winters as well, while storm tracks southward toward the Mediterranean Sea. Therefore, the reported winter decadal variability of WS across Sweden can to a large extent be explained by the NAO index, with the positive NAO index trend forcing an increase in winter WS.

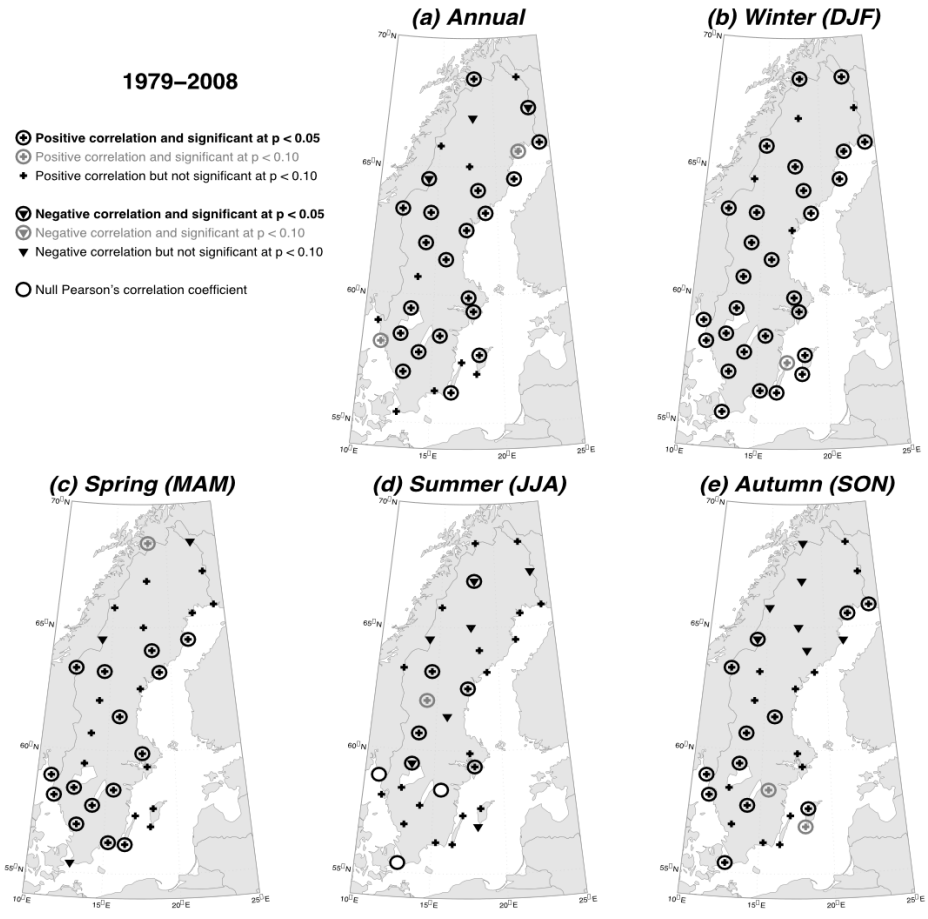

Figure 22. Spatial distribution of the sign and significance of Pearson's correlation relationship between the wind speed anomalies (m s^{-1}) and the NAO index on the annual and seasonal bases for 1979-2008 (33 stations) (Figure 8 from Paper V).

In Paper VI, we look for whether a similar slowdown continues over recent decades (1997-2019) or, as shown by Zeng et al. (2019) over Europe, East Asia and North America, a reversal in the terrestrial stilling can be detected. Comparison between 1956-2013 and 1997-2019 WS series shows that the significant slowdown in WS observed since ~1990 (which is dominated by the winter variability) is followed by a non-significant recovery trend from around 2003 (Figure 22 and Figure 24). Specifically, a stabilization in wind change is observed during 2003-2010; afterwards the winds slightly increase during 2010-2014; and a new slowdown starts since 2014. Even though an overall WS decline was observed during 1956-2013, no evident trend is detected since around 2003 and a recovery from previous years slowdown is observed. This is in line with the stilling-reversal detected in terrestrial midlatitude regions (Kim & Paik 2015; Azorin-Molina et al. 2018a; Zhang & Wang 2020).

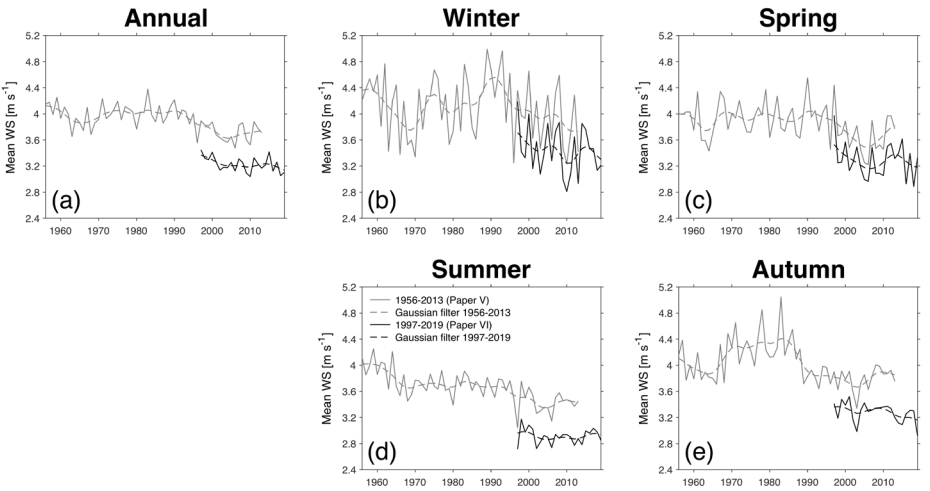

Figure 23. Series of mean annual and seasonal WS for Sweden during 1997-2019 (from Paper VI; black line) and during 1956-2013 (from Paper V; grey line). The low-frequency variability is shown with the dashed lines of the applied Gaussian-weighted average filter (modified Figure 6 from Paper VI).

Similar to DAWS, the DPWG also underwent four changing phases during 1997-2019, i.e., an early slowdown, stabilization, recovery, and recent slowdown Figure 24). The overall agreement in variability between mean and gust wind speeds is consistent with what observed over the Iberian Peninsula by Azorin-Molina et al. (2016), demonstrating that local-to-regional weather systems and teleconnection patterns with synoptic features are needed to understand wind dynamics across Sweden.

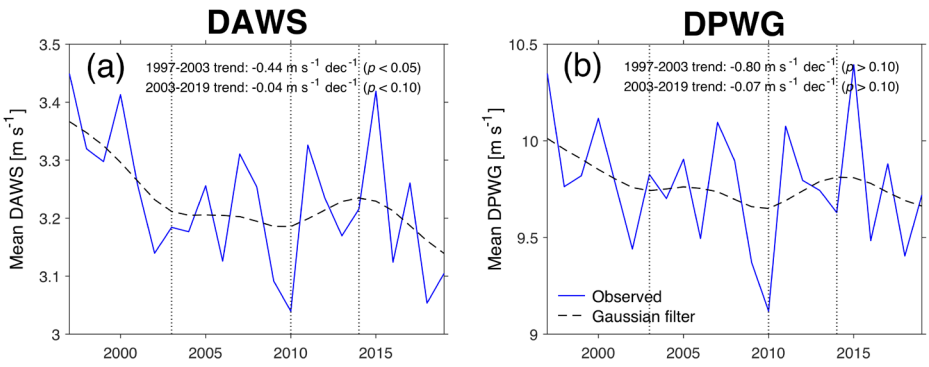

Figure 24. Series of mean annual DAWS (right) and DPWG (left) for Sweden from 1997 to 2019. The low-frequency variability is shown with the black dashed lines of the applied Gaussian-weighted average (modified Figure 2 from Paper VI).

As the decadal variabilities of both DAWS and DPWG are significantly correlated with the NAO index during winter, the recovery in the wind stilling is mostly due to the large-scale circulation changes associated with the NAO (Figure 25). This agrees with what previously observed by Azorin-Molina et al. (2018a) over Saudi Arabia or by Kim and Paik (2015) over South Korea. Climate model simulations confirm the impact of large-scale circulation in the wind reversal detected since around 2010, when global surface wind speed trends shifted in their sign, as presented in Paper I (see Section 5.1).

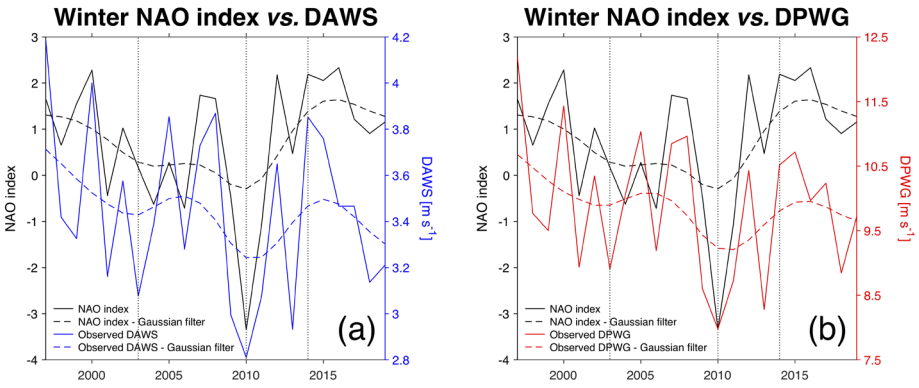

Figure 25. Series of winter NAO index *vs.* observed mean winter DAWS (left) and DPWG (right) for 1997-2019. The low-frequency variability is shown with the dashed lines of the applied Gaussian-weighted average (Figure 9 from Paper VI).

In addition to the NAO, the extratropical cyclone activities are also examined to better understand the decadal wind variability across Sweden. In fact, extratropical cyclones, growing through baroclinic instability, cause severe weather events including heavy precipitation and strong near-surface winds (Belusic et al. 2019). Previous studies have shown a major cyclone activities area over the North Atlantic Ocean and northwestern Europe (Hoskins & Hodges 2002), and extratropical cyclones from these regions have a large influence on storminess in Sweden (Belusic et al. 2019). In Paper VI, near-surface wind observations provide evidence of the influence of intensity changes of such low-pressure systems on winter surface winds, especially when it comes to the wind gusts strength (Figure 26). The majority of the observed DPWG series display a strong and significant ($p < 0.05$) correlation with the intensity of extratropical cyclones. Note that, as intensity refers to SLP anomaly, negative correlation indicates a stronger wind when a stronger cyclone passes. Most importantly, cyclone intensity change agrees well with the wind slowdown observed until 2003 and the absence of a clear trend afterwards, indicating both the large-scale circulation associated with the NAO and extratropical cyclones (which are also partly influenced by the NAO; Keim et al. 2004) play a key role in the detected wind stilling-reversal across Sweden.

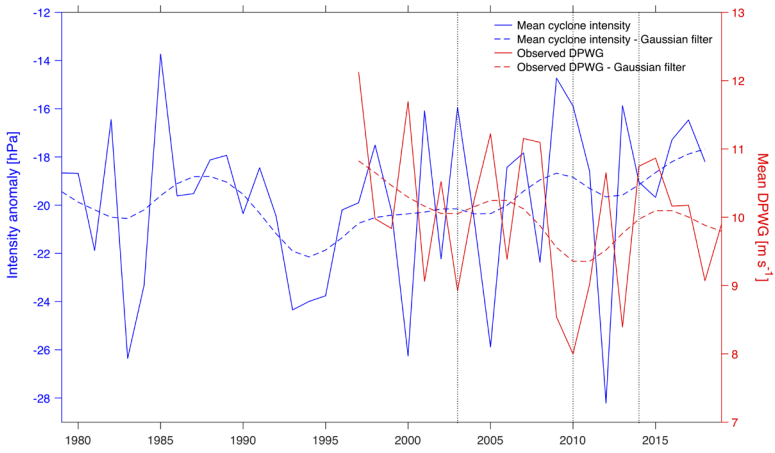

Figure 26. Series of mean winter cyclone intensity (1979-2018; blue line) and DPWG (1997-2019; red line). The low-frequency variability is shown with the dashed lines of the applied Gaussian-weighted average. Mean series are calculated only using stations that show significant (at $p < 0.05$) negative correlation between winter cyclone intensity and DPWG series (modified Figure 10 from Paper VI).

Besides the large-scale atmospheric circulation dominating wind variability across Sweden (and driving the stilling-recovery), the impact of surface roughness changes is also explored as a possible reason of the observed variability (see Equation 1 in Section 2.1). Figure 27 illustrates both observed and ERA5 annual wind series for 1997-2019. ERA5 winds follow well the observed variability (correlation higher than 0.8 and significant at $p < 0.05$), displaying the four phases in wind changes. Even though ERA5 wind series correlate well with the observations, they do not show a general slowdown, with trends overall "more negative" for the observations compared to ERA5. By design, reanalysis products do not include in their hindcasting the changes in surface roughness (Thorne & Vose 2010). For this reason, land-use changes can explain such differences.

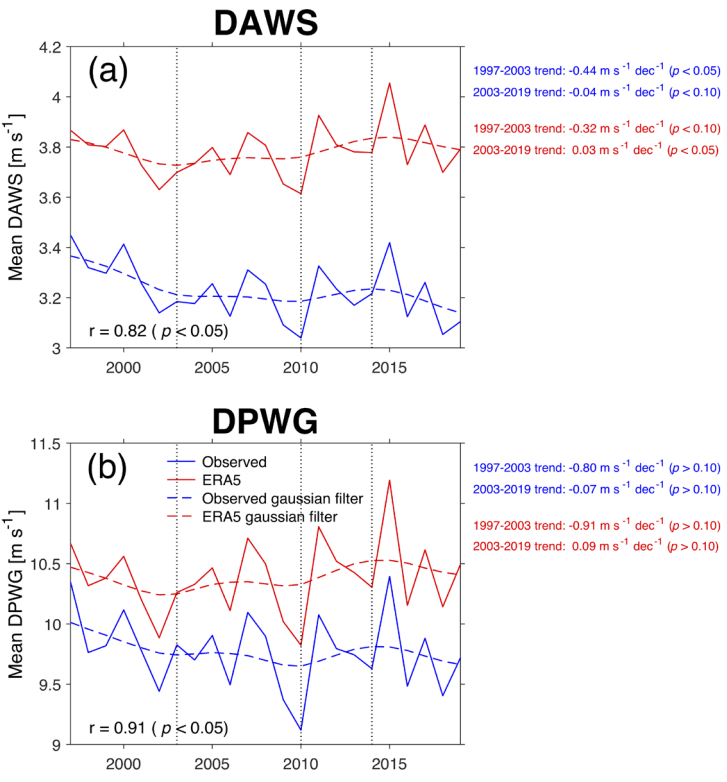

Figure 27. Comparison of observed (blue) and ERA5 (red) mean annual DAWS (left) and DPWG (right) series for Sweden from 1997-2019. The low-frequency variability is shown by applying a Gaussian-weighted average (dashed lines) (modified Figure 12 from Paper VI).

Increase of surface roughness can be associated with factors such as urbanization, growth of forests, changes in trees and forest distribution or changes in agricultural practices (Yupeng et al. 2019). Previous studies have mainly focused on land-use changes induced by urbanization, with comparison between urban and rural stations (Chen et al. 2020). In Paper VI we evaluate how wind speed long-term trends can be impacted by surface roughness changes associated with forest cover modifications.

Independent of how the landscape is in the proximity of a station (e.g., urban, inland, coastal, etc.), change in forest cover is the main modification that can be detected in the surroundings during the period considered. An increase (or decrease) of forest cover and forest growth in proximity to the station surrounding over years affects the exposure of the measuring instrument. Consequently, a decrease (or increase) in recorded wind arises from the artificial change of surface roughness in the weather station proximity. Forest cover changes in the proximity of weather stations indeed show a moderate but linear relationship with annual DAWS (Figure 28), indicating that the overall wind slowdown during 1997-2019 is likely partly caused by forest cover increase.

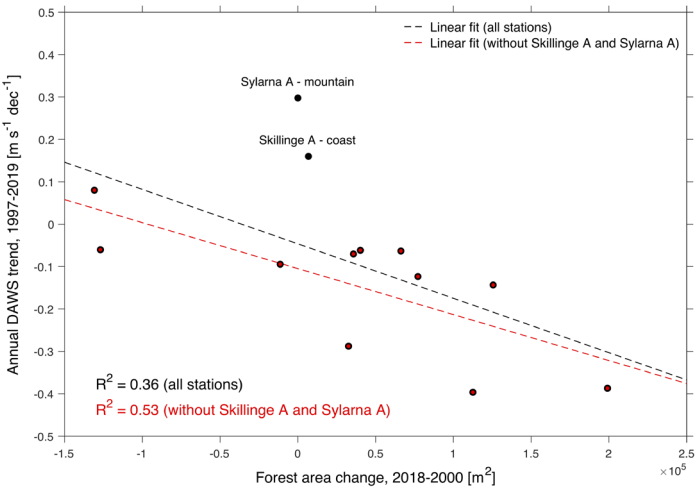

Figure 28. Relationship between forest area change (in m^2) between 1998-2018 in a 1 x 1 km area around the weather station, and annual DAWS trend during 1997-2019 for 13 selected weather stations. The black dashed line is the linear fit calculated using all the 13 stations; the red dashed line is the linear fit calculated excluding Skillinge A and Sylarna A stations (Figure 15 from Paper VI).

To summarize, changes in terrestrial near-surface winds can be induced by a combination of different causes, from anthropogenic activities to natural climate changes. In Paper V and Paper VI, atmospheric circulation associated with the NAO and cyclone activity changes are confirmed to be the driving factor behind the stilling and the recent recovery of surface winds across Sweden, in line with what observed across different midlatitude regions (Kim and Paik 2015; Azorin-Molina et al. 2018a; Zeng et al. 2019). The observed reduction of surface wind speed is also partly attributed to land use and cover change, as similarly shown by Vautard et al. (2010) and Wever (2012). Notice that Paper V and Paper VI only qualitatively relate decadal wind variability to both atmospheric circulation and surface roughness changes. Future work should quantify and distinguish the sources of these changes in the driving forces (Wu et al. 2018).

When relating the Lagrangian form of the wind equation (Equation 1 in Section 2.1) to the observed wind variability, we can conclude that:

- large-scale atmospheric circulation (i.e., NAO) and synoptic weather systems (i.e., extratropical cyclones) are responsible to changes in the pressure gradient forcing $\vec{G}$ (i.e., the atmospheric motion), driving the slowdown and stilling-reversal;

- increase in forest cover does increase the drag force $\vec{f}$, partly contributing to the surface wind slowdown observed across Sweden.

Therefore, if we are to make accurate predictions of regional wind change across Sweden, it is important to understand how both these two forces will vary in the future. Future changes in surface roughness will be largely affected by the human impact on land-use (e.g., urbanization or replacing of forests in agricultural fields), but they are also related to how the environment will respond to a warmer climate (e.g., desertification and greening; Burrel et al. 2020; Pausata et al. 2020). Right now, future projections of land-use changes across Sweden are unclear. When it comes to NAO, even though it is a natural mode of atmospheric variability, surface, stratospheric or even anthropogenic processes (e.g., increase in greenhouse gases concentration) may influence its phase and amplitude of variation (Visbeck et al. 2001; Gillet et al. 2003). At present, there is no consensus on the mechanisms that are responsible for the observed multidecadal variations in NAO. This is reflected by climate models

which lack ability to simulate NAO variability and leave us uncertain about how NAO will change in the future (Deser et al. 2017). This also implies substantial uncertainty in regional winds across Sweden over the coming decades. Similarly, there is no clear evidence of multidecadal trends in cyclone frequency or intensity; instead, cyclone location, frequency and intensity showed considerable decadal variability over the past century (Feser et al. 2015; Füssel et al. 2017). There is low confidence in the response of the North Atlantic cyclone statistics to global warming, with model-projections unclear on their possible future evolutions (Christensen et al. 2013). For example, as the sign of NAO strongly impacts the frequencies and location of these systems (Keim et al. 2004) and with absence of clear long-term trends in the NAO pattern, it is uncertain how the magnitude of cyclone frequency and intensity will vary under different future scenarios. Therefore, it is also unclear how wind extremes associated with deep low-pressure systems will change in a warmer climate.

6 Conclusions

Because of the large impact of near-surface winds on humans and ecosystems, it is necessary to understand the mechanisms behind their origins, so that their possible future changes can be reliable projected and the society can adapt to the wind conditions of a warmer climate. In this context, this thesis focuses on both surface mean and gust wind speeds across Sweden. By analyzing meteorological observations and climate model outputs, it aims to identify the physical processes behind their origin and attribute past wind changes. In particular, a dataset of observed wind speed series is constructed for the first time across Sweden by homogenizing in-situ measurements. This dataset is used to identify the climatological features of observed winds, which current regional climate models and reanalyses cannot not fully simulate (i.e., winds over the complex topography of the Scandes). A better simulation of surface wind gusts is achieved when the mechanisms responsible of gustiness are better parametrized by implementing an elevation-dependency and by tuning the convective gust contribution. Observed wind series do not show a clear linear trend during the past decades. Instead, in line with what is shown globally by reanalysis and climate models, the wind decline observed until 2003 is followed by no clear trend afterwards. The detected stilling-reversal is linked to large-scale atmospheric circulation changes, in particular to the NAO and the intensity changes of extratropical cyclones passing across Sweden. But the background slowdown detected in most stations does not appear in the reanalysis data, revealing that, in addition to the large-scale interannual variability, changes in surface roughness (e.g. changes in forest cover) contribute to explain the observed wind variability.

Therefore, two forcing are identified as the key factors responsible for the observed wind changes across Sweden.: (i) large-scale atmospheric circulation changes, in particular the North Atlantic Oscillation and the intensity changes of extratropical cyclones passing across Sweden, are linked to the detected stilling-reversal; and (ii) surface roughness modifications, related for example to forest cover changes, contribute to explaining the observed wind stilling. Consequently, to make accurate predictions of regional wind change across Sweden and thus understand their future impacts, it is important to understand how both these two forces will vary in the future.

The main conclusions of this thesis can be summarized as follows.

- The longest available near-surface mean (1956-2019) and gust (1996-2019) wind speed dataset is created for Sweden by applying a robust homogenization protocol (Paper III, Paper V & Paper VI).

- Wind gust measurements across Sweden carried with a 2 s gust duration differ by 3% - 7% for high turbulence intensities and by 1% - 3% at low intensities compared to gusts recorded with a 3 s duration, as recommended by WMO (Paper I).

- The observed climatology of wind gust is explored for Sweden. According to them, meteorological stations are classified into three regions for which wind conditions are driven by similar physical processes: coast, inland, and mountain (Paper III).

- Both the analyzed RCMs and reanalyses show fair skills in simulating wind gusts over coastlines, but not in inland and mountainous regions. This calls for an even higher resolution and better representation of relevant physical processes (i.e., needs of a better gust parametrization) (Paper III & Paper IV).

- Wind gusts can be better simulated by ERA5 when in the gust parametrization an elevation dependency is implemented for the turbulent contribution and the convective gust term is tuned to the observed climatologies (Paper IV).

- In line with the global changes in near-surface winds detected in reanalyses and climate models, a break in the stilling is identified around 2003 across Sweden. The observed stilling-reversal is possibly linked to the recent changes in large-scale atmospheric circulation features, such as NAO and cyclone activity (Paper I, Paper V & Paper VI).

- Even with atmospheric circulation driving most of the wind variability across Sweden, forest cover increase detected in the weather stations surrounding has also contributed to decreasing wind trends, as a background slowdown not found in the ERA5 reanalysis. Modifications in surface roughness, together with large-scale atmospheric changes, are the two dominating factors explaining most of the observed near-surface wind variability across Sweden (Paper VI).

References

Abhishek A., Lee J.-Y., Keener T. C., & Yang Y. J. (2012): Long-term wind speed variations for three midwestern U.S. cities. *Journal of the Air & Waste Management Association*, **60** (9), 1057-1064. https://doi.org/10.3155/1047-3289.60.9.1057

Achberger C., Chen D., & Alexandersson A. (2006): The surface winds of Sweden during 1999-2000. *International Journal of Climatology*, **26** (2), 159-178. https://doi.org/10.1002/joc.1254

Aguilar E., Auer I., Brunet M., Peterson T. C., & Wiering J. (2003): Guidelines on climate metadata and homogenization. WMO Technical Document (No. 1186). https://library.wmo.int/index.php?lvl=notice_display&id=11635#.XmqUtlAo8dV

Alexandersson H., (1986): A homogeneity test applied to precipitation data. *Journal of Climatology*, **6** (6), 661-675. https://doi.org/10.1002/joc.3370060607

Alexandersson H. (2006): Vindstatistik för Sverige 1961-2004. Meteorologi 121. http://www.smhi.se/polopoly_fs/1.1895!/meteorologi_121-06%5B1%5D.pdf

American Meteorological Society (AMS) (2013): Regional climate model. Glossary of Meteorology. https://glossary.ametsoc.org/wiki/Regional_climate_model

Anthes R. A. (1985): Introduction to parametrization of physical processes in numerical models. Seminar on physical parametrization for numerical models of the atmosphere, Shinfield Park, Reading, 9-13 September, ECMWF. https://www.ecmwf.int/en/elibrary/7786-introduction-parameterization-physical-processes-numerical-models

Arya S. P. (2001): Introduction to micrometeorology, 2nd Edition. Academic Press, San Diego, pp. 420

Azorin-Molina C., and Coauthors (2014): Homogenization and assessment of observed near-surface wind speed trends over Spain and Portugal, 1961-2011. *Journal of Climate*, **27** (10), 3692-3712. https://doi.org/10.1175/JCLI-D-13-00652.1

Azorin-Molina C., Guijarro J. A., McVicar T. R., Vicente-Serrano S. M., Chen D., Jerez S., & Espírito-Santo F. (2016): Trends of daily peak wind gusts in Spain and Portugal, 1961-2014. *Journal of Geophysical Research – Atmospheres*, **121** (3), 1059-1078. https://doi.org/10.1002/2015JD024485

Azorin-Molina C., Rehman S., Guijarro J. A., McVicar T. R., Minola L., Chen D., & Vicente-Serrano S. M. (2018a): Recent trends in wind speed across Saudi Arabia, 1978-2013: a break in the stilling. *International Journal of Climatology*, **38** (S1), e966-e984. https://doi.org/10.1002/joc.5423

Azorin-Molina C., Asin J., McVicar T. R., Minola L., Lopez-Moreno J. I., Vicente-Serrano S. M., & Chen D. (2018b): Evaluating anemometer drift: A statistical approach to correct biases in wind speed measurement. *Atmospheric Research*, **203**,175-188. https://doi.org/10.1016/j.atmosres.2017.12.010

Azorin-Molina C., Guijarro J. A., McVicar T. R., Trewin B. C., Frost A. J., & Chen D. (2019): An approach to homogenize daily peak wind gusts: An application to the Australian series. *International Journal of Climatology*, **39**, 2260-2277. https://doi.org/10.1002/joc.5949

Belusic D., and Coauthors (2019): Climate extremes for Sweden. SMHI Report. http://smhi.diva-portal.org/smash/get/diva2:1368107/FULLTEXT01.pdf

Beniston, and Coauthors (2007): Future extreme events in European climate: an exploration of regional climate projections. *Climate change*, **81**, 71-95. https://doi.org/10.1007/s10584-006-9226-z

Betchtold P., & Bidlot J. R. (2009): Parametrization of convective gusts. *ECMWF Newsletter*, **199**, 15-18. https://doi.org/10.21957/kfr42kfp8c

Borne K., Chen D., & Nunez M. (1998): A method for finding sea breeze days under stable synoptic conditions and its application to the Swedish west coast. *International Journal of Climatology*, **18** (6), 901-914. https://doi.org/10.1002/(SICI)1097-0088(19980630)18:8<901::AID-JOC295>3.0.CO;2-F

Boucher O., Denvil S., Caubel A., & Foujols M. A. (2018): IPSL IPSL-CM6A-LR model output prepared for CMIP6 CMIP. *Earth System Grid Federation*. https://doi.org/10.22033/ESGF/CMIP6.1534

Brasseur O. (2001): Development and application of a physical approach to estimate wind gusts. *Monthly Weather Research*, **129** (1), 5-25. https://doi.org/10.1175/1520-0493(2001)129<0005:DAAOAP>2.0.CO;2

Brázdil R., Hostýnek J., Řezníčková L., Zahradníček P., Tolasz R., Dobrovolný P., & Štěpánek P. (2017): The variability of maximum wind gusts in the Czech Republic between 1961 and 2014. *International Journal of Climatology*, **37** (4), 1961-1978. https://doi.org/10.1002/joc.4827

Burrell A. L., Evans J. P., & De Kauwe M. G. (2020): Anthropogenic climate change has driven over 5 million km^2 of drylands towards desertification. *Nature Communications*, **11**, 3853. https://doi.org/10.1038/s41467-020-17710-7

Chen D. (2000): A monthly circulation climatology for Sweden and its application to a winter temperature case study. *International Journal of Climatology*, **20** (10), 1067-1076. https://doi.org/10.1002/1097-0088(200008)20:10<1067::AID-JOC528>3.0.CO;2-Q

Chen D., & Hellström, C. (1999): The influence of the North Atlantic Oscillation on the regional temperature variability in Sweden: spatial and temporal variations. *Tellus*, **51A**, 505-516. https://doi.org/10.3402/tellusa.v51i4.14086

Chen X., Jeong, S., Park H., Kim J., & Park C.-R. (2020): Urbanization has stronger impacts than regional climate change on wind stilling: a lesson from South Korea. *Environmental Research Letters*, **15**, 054016. https://doi.org/10.1088/1748-9326/ab7e51

Christensen J.H., and Coauthors (2013): Climate Phenomena and their Relevance for Future Regional Climate Change. In *Climate Change 2013: The Physical Science Basis*. Cambridge University Press, Cambridge and New York, pp. 1217-1308

Cohen A. E., Coniglio M. C., Corfidi S. F., & Corfidi A. J. (2007): Discrimination of mesoscale convective system environments using sounding observations. *Weather and Forecasting*, **22** (5), 1045-1062. https://doi.org/10.1175/WAF1040.1

Cohen J., and Coauhtors (2020): Divergent consenses on Arctic amplification influence on midlatitude severe winter weather. *Nature Climate Change*, **10**, 20-29. https://doi.org/10.1038/s41558-019-0662-y

Collins M., and Coauthors (2013): Long-term climate change: Projections, commitments and irreversibility. In *Climate change 2013: The physical science basis. Contribution of Working Group I to the Fifth Assessment Report of the Intergovernmental Panel on Climate Change*. Cambridge University Press, Cambridge, pp. 1029-1136

Coumou D., Lehmann J., & Beckmann J. (2015): The weakening summer circulation in the Northern Hemisphere mid-latitudes. *Science*, **348** (6232), 324-327. https://doi.org/10.1126/science.1261768

Cusack S. (2013): A 101 year record of windstorms in the Netherlans. *Climatic Change*, **116**, 693-704. https://doi.org/10.1007/s10584-012-0527-0

Davenport A. G. (1964): Note on the distribution of the largest value of a random function with application to gust loading. *Proceedings of the Institution of Civil Engineers*, **28** (2), 187-196. https://doi.org/10.1680/iicep.1964.10112

Dee D. P., and Coauthors (2011): The ERA-Interim reanalysis: configuration and performance of the data assimilation system. *Quarterly Journal of Royal Meteorological Society*, **137** (656), 553-597. https://doi.org/10.1002/qj.828

Deser C., Hurrell J. W., & Phillips A. S. (2017): The role of the North Atlantic Oscillation in European climate projections. *Climate Dynamics*, **49**, 3141-3157. https://doi.org/10.1007/s00382-016-3502-z

Déqué M., and Coauthors (2007): An intercomparison of regional climate simulations for Europe: assessing uncertainties in model projections. *Climatic Change*, **81**, 53-70. https://doi.org/10.1007/s10584-006-9228-x

European Center for Medium-Range Weather Forecasts (ECMWF) (2016): IFS Documentation CY45R2 – Part IV: Physical processes. IFC Documentation. https://www.ecmwf.int/en/elibrary/16648-part-iv-physical-processes

European Center for Medium-Range Weather (ECMWF) (2020): ERA5 data documentation – Observations. https://confluence.ecmwf.int/display/CKB/ERA5%3A+data+documentation#ERA5:datadocumentation-Observations

Eyring V., Bony S., Meehl G. A., Senior C. A., Stevens B., Stouffer R. J., & Taylor K. E. (2016): Overview of the Coupled Model Intercomparison Project Phase 6 (CMIP6) experimental design and organization. *Geoscientific Model Development*, **9**, 1937-1958. https://doi.org/10.5194/gmd-9-1937-2016

Feser F., Barcikowska M., Krueger O., Schenk F., Weisse R., & Xia L. (2015): Storminess over the North Atlantic and northwestern Europe – A review. *Quarterly Journal of the Royal Meteorological Society*, **141** (687), 350-382. https://doi.org/10.1002/qj.2364

Fujii T. (2007): On geographical distributions and decadal changes of the annual maximum wind speeds caused by typhoons in Japan. *Journal of Natural Disaster Science*, **26**, 267-277.

Füssel H.-M., Jol A., Marx A., & Hildén M. (2017): Climate change, impacts and vulnerability in Europe 2016 – An indicator-based report. EEA Report 1. https://climate-adapt.eea.europa.eu/metadata/publications/climate-change-impacts-and-vulnerability-in-europe-2016/climate-change-impacts-and-vulnerabilities-2016-thal17001enn.pdf

Gelaro R., and Coauthors (2017): The Modern Era-Retrospective analysis for Research and Applications, version 2 (MERRA-2). *Journal of Climate*, **30** (14), 5419-5454. https://doi.org/10.1175/JCLI-D-16-0758.1

Gillet N. P., Graf H. F., & Osborn T. J. (2003): Climate change and the North Atlantic Oscillation. In *The North Atlantic Oscillation: Climatic significance and environmental impact*. AGU, Washington, pp. 193-209. https://doi.org/10.1029/134gm09

Giorgi F., Jones C., & Asrar G. R. (2009): Addressing climate information needs at the regional level: the CORDEX framework. WMO Bulletin 58 (3). https://public.wmo.int/en/bulletin/addressing-climate-information-needs-regional-level-cordex-framework

Global Destinations Sustainability Movement (2019): Gothenburg, Sweden. https://www.gds.earth/destination/Gothenburg/2019/

Grundström M., Linderholm H. W., Klingberg J., & Pleijel H. (2011): Urban NO_2 and NO pollution in relation to the North Atlantic Oscillation NAO. *Atmospheric Environment*, **45** (4), 883-888. https://doi.org/10.1016/j.atmosenv.2010.11.023

Grundström M., Hak C., Chen D., Hallquist M., & Pleijel H. (2015): Variation and co-variation of PM10, particle number concentration, NOx and NO2 in the urban air – Relationships with wind speed, vertical temperature gradient and weather type. *Atmospheric Environment*, **120**, 317-327. https://doi.org/10.1016/j.atmosenv.2015.08.057

Guijarro J. A. (2017): Daily series homogenization and gridding with Climatol v.3. In *Ninth Seminar for Homogenization and Quality control in Climatological Databases and Fourth Conference on Spatial Interpolation Techniques in Climatology and Meteorology*. WMO, Budapest, Hungary, pp. 175-180 https://library.wmo.int/doc_num.php?explnum_id=5680

Guijarro J. A. (2018): Homogenization of climatic series with Climatol. http://www.climatol.eu/homog_climatol-en.pdf

Gustavsson T., Lindqvist S., Borne K., & Bogren J. (1995): A study of sea and land breezes in an archipelago on the west coast of Sweden. *International Journal of Climatology*, **15** (7), 785-800. https://doi.org/10.1002/joc.3370150706

Haanpää S., Lehtonen S., Peltonen L., & Talockaite E. (2007): Impacts of winter storm Gudrun of 7th – 9th January 2005 and measures taken in Baltic Sea Region. ASTRA project Report. https://discomap.eea.europa.eu/map/Data/Milieu/OURCOAST_110_Baltic/OURCOAST_110_Baltic_Doc1_ImpactGudrunStorm.pdf

Hack J. J., Schubert W. H., Stevens D. E., & Kuo H.-C. (1989): Response of the Hadley circulation to convective forcing in the ITCZ. *Journal of the Atmospheric Sciences*, **46** (19), 2957-2973. https://doi.org/10.1175/1520-0469(1989)046<2957:ROTHCT>2.0.CO;2

Hannon Bradshaw L. (2017): Sweden, forests and wind storms: developing a model to predict storm damage to forests in Kronoberg County. Master's thesis, Lund University. http://lup.lub.lu.se/student-papers/record/8908951

Hanssen-Bauer I, & Førland E. (2000): Temperature and precipitation variations in Norway 1900-1994 and their links to atmospheric circulation. *International Journal of Climatology*, **20** (14), 1693-1709. https://doi.org/10.1002/1097-0088(20001130)20:14<1693::AID-JOC567>3.0.CO;2-7

Hartmann B., & Wendler G. (2005): The significance of the 1976 Pacific climate shift in the climatology of Alaska. *Journal of Climate*, **18** (22), 4824-4839. https://doi.org/10.1175/JCLI3532.1

Helbig N., Mott R., van Herwijnen A., Winstral A., & Jonas T. (2017): Parameterizing surface wind speed over complex topography. *Journal of Geophysical Research: Atmospheres*, **122**, 651-667. https://doi.org/10.1002/2016JD025593

Hersbach H., and Coauthors (2018): Operational global reanalysis: progress, future directions and synergies with NWP. ERA Report Series 27. https://www.ecmwf.int/en/elibrary/18765-operational-global-reanalysis-progress-future-directions-and-synergies-nwp

Hoskins B. J., & Hodges, K. I. (2002): New perspectives on the Northern Hemisphere winter storm tracks. *Journal of the Atmospheric Sciences*, **59** (6), 1041-1061. https://doi.org/10.1175/1520-0469(2002)059<1041:NPOTNH>2.0.CO;2

Hurrell J. W. (1995): Decadal trends in the North Atlantic Oscillation: regional temperatures and precipitation. *Science*, **269** (5224), 676-679. https://doi.org/10.1126/science.269.5224.676

Hurrell J. W., & van Loon, H. (1997): Decadal variations in climate associated with the North Atlantic Oscillation. *Climatic Change*, **36**, 301-326. https://doi.org/10.1023/A:1005314315270

Intergovernmental Panel on Climate Change (IPCC) (2014): Climate Change 2014: Synthesis Report. Contribution of Working Groups I, II, and III to the Fifth Assessment Report of the Intergovernmental Panel on Climate Change. IPCC, Geneva, Switzerland, pp. 151

Intergovernmental Panel on Climate Change (IPCC) (2018): What is a GCM? https://www.ipcc-data.org/guidelines/pages/gcm_guide.html

Jeong J.-H., Walther A., Nikulin G., Chen D., & Jones C. (2011): Diurnal cycle of precipitation amount and frequency in Sweden: observation vs model simulation. *Tellus A*, **63** (4), 664-674. https://doi.org/10.1111/j.1600-0870.2011.00517.x

Jeong I. D., & Sushama L. (2019): Projected changes to mean and extreme surface wind speeds for North America based on regional climate model simulations. *Atmosphere*, **10** (9), 497. https://doi.org/10.3390/atmos10090497

Jiménez P. A., & Dudhia J. (2012): Improving the representation of resolved and unresolved topographic effects on surface wind in the WRF model. *Journal of Applied Meteorology and Climatology*, **51** (2), 300-316. https://doi.org/10.1175/JAMC-D-11-084.1

Johns R. H., & Doswell C. A. (1992): Severe local storms forecasting. *Weather and Forecasting*, **7** (4), 588-612. https://doi.org/10.1175/1520-0434(1992)007<0588:SLSF>2.0.CO;2

Jones P. D., Jonsson, T., & Wheeler, D. (1997): Extension of the North Atlantic oscillation using early instrumental pressure observations from Gibraltar and south-west Iceland. *International Journal of Climatology*, **17** (13), 1433-1450. https://doi.org/10.1002/(SICI)1097-0088(19971115)17:13<1433::AID-JOC203>3.0.CO;2-P

Jönsson P., & Fortuniak K. (1995): Interdecadal variations of surface wind direction in Lund, southern Sweden, 1741-1990. *International Journal of Climatology*, **15** (4), 447-461. https://doi.org/10.1002/joc.3370150407

Kanamitsu M., Ebisuzaki W., Woollen J., Yang S.-K., Hnilo, J. J., Fiorino M., & Potter G. L. (2002): NCEP-DOE AMIP-II Reanalysis (R-2). *Bulletin of the American Meteorological Society*, **83** (11), 1631-1644. https://doi.org/10.1175/BAMS-83-11-1631

Kang S. M., Seager R., Frierson D. M. W., & Liu X. (2015): Croll revisited: Why is the northern hemisphere warmer than the southern hemisphere? *Climate Dynamics*, **44**, 1457-1472. https://doi.org/10.1007/s00382-014-2147-z

Keim B. D., Muller, R. A., & Stone, G. W. (2004): Spatial and temporal variability of coastal storms in the North Atlantic Basin. *Marine Geology*, **210**, 7-15. https://doi.org/10.1016/j.margeo.2003.12.006

Kendon E. J., and Coauthors (2017): Do convection-permitting regional climate models improve projections of future precipitation change? *Bulletin of the American Meteorological Society*, **83** (1), 79-93. https://doi.org/10.1175/BAMS-D-15-0004.1

Kim J., & Paik K. (2015): Recent recovery of surface wind speed after decadal decrease: a focus on South Korea. *Climate Dynamics*, **45**, 1699-1712. https://doi.org/10.1007/s00382-015-2546-9

Kjellström E., and Coauthors (2005): A 140-year simulation of European climate with the new version of the Rossby Centre regional atmospheric climate model (RCA3). SMHI Reports Meteorology and Climatology 108. https://www.smhi.se/polopoly_fs/1.2104!/RMK108%5B1%5D.pdf

Klink K. (2015): Seasonal patterns and trends of fastest 2-min winds at coastal stations in the conterminous USA. *International Journal of Climatology*, **35** (14), 4167-4175. https://doi.org/10.1002/joc.4275

Kobayashi S., and Coauthors (2015): The JRA-55 reanalysis: General specifications and basic characteristics. *Journal of the Meteorological Society*, **93** (1), 5-48. https://doi.org/10.2151/jmsj.2015-001

Kunz M., Mohr S., Rauthe M., Lux R., & Kottmeier Ch. (2010): Assessment of extreme wind speeds from Regional Climate Models – Part 1: Estimation of return values and their evaluation. *Natural Hazards and Earth System Sciences*, **10**, 907-922. https://doi.org/10.5194/nhess-10-907-2010

Kwon D. K., & Kareem A. (2014): Revisiting gust averaging time and gust effect factor in ASCE 7. *Journal of Structural Engineering*, **140** (11). https://doi.org/10.1061/(ASCE)ST.1943.541X.0001102

Landberg L. (2016): Meteorology for wind energy – An introduction. John Wiley & Sons Ltd, Chichester, pp. 204

Lin C., Yang K., Qin J., and Fu R. (2013): Observed coherent trends of surface and upper-air wind speed over China since 1960. *Journal of Climate*, **26** (9), 1891-2903. https://doi.org/10.1175/JCLI-D-12-00091.1

Linderholm H. W., and Coauthors (2011): Interannual teleconnections between the summer North Atlantic Oscillation and the East Asian summer monsoon. *Journal of Geophysical Research – Atmospheres*, **116** (D13). https://doi.org/10.1029/2010JD015235

Lynch A. H., Curry J. A., Brunner R. D., & Maslanik J. A. (2004): Toward an integrated assessment of the impact of extreme wind events on Barrow, Alaska. *Bulletin of the American Meteorological Society*, **85** (2), 209-222. https://doi.org/10.1175/BAMS-85-2-209

L'Heureux M. L., Sukyoung L., & Lyon B. (2013): Recent multidecadal strengthening of the Walker circulation across the tropical Pacific. *Nature Climate Change*, **3**, 571-576. https://doi.org/10.1038/nclimate1840

Martyn D. (1992): Climates of the Worlds. Elsevier, Amsterdam, pp. 436

McGee D., Donohoe A., Marshall J., & Ferreira D. (2014): Changes in the ITCZ location and cross-equatorial heat transport at the Last Glacial Maximum, Heinrich Stadial 1, and the mid-Holocene. *Earth and Planetary Science Letter*, **390**, 69-79. https://doi.org/10.1016/j.epsl.2013.12.043

McVicar T. R., and Coauthors (2012a): Global review and synthesis of trends in observed near-surface wind speeds: Implications for evaporation. *Journal of Hydrology*, **416-417**, 182-2005. https://doi.org/10.1016/j.jhydrol.2011.10.024

McVicar T. R., Roderick M. L., Donohue R. J., & Van Niel T. G. (2012b): Less bluster ahead? Ecohydrological implications of global trends of terrestrial near-surface wind speeds. *Ecohydrology*, **5** (4), 381-388. https://doi.org/10.1002/eco.1298

Met Office (2018): North Atlantic Oscillation. https://www.metoffice.gov.uk/weather/learn-about/weather/atmosphere/north-atlantic-oscillation

Miao H., Dong D., Huang G., Hu K., Tian Q., & Gong Y. (2020): Evaluation of Northern Hemisphere surface wind speed and wind power density in multiple reanalysis datasets. *Energy*, **200**, 117382. https://doi.org/10.1016/j.energy.2020.117382

National Oceanic and Atmospheric Administration (NOAA) (2012): North Atlantic Oscillation (NAO). https://www.cpc.ncep.noaa.gov/data/teledoc/nao.shtml

National Oceanic and Atmospheric Administration (NOAA) (2018): Turbulence. https://www.weather.gov/source/zhu/ZHU_Training_Page/turbulence_stuff/turbulence/turbulence.htm

Nikulin G., Kjellström E., Hansson U., Strandberg G., & Ullerstig A. (2010): Evaluation and future projection of temperature, precipitation and wind extremes over Europe in an ensemble of regional climate simulations. *Tellus*, **63** (1), 41-55. https://doi.org/10.1111/j.1600-0870.2010.00466.x

Panofsky H. A., Tennekes H., Lenschow D. H., & Wyngaards J. C. (1977): The characteristics of turbulent velocity components in the surface layer under convective conditions. *Boundary-Layer Meteorology*, **11**, 355-361. https://doi.org/10.1007/BF02186086

Pausata F. S.R., and Coauthors (2020): The greening of the Sahara: Past changes and future implications. *One Earth*, **2** (3), 235-250. https://doi.org/10.1016/j.oneear.2020.03.002

Poli P., and Coauthors (2016): ERA-20C: An atmospheric reanalysis of the twentieth century. *Journal of Climate*, **29** (11), 4083-4097. https://doi.org/10.1175/JCLI-D-15-0556.1

Prein A. F., and Coauthors (2015): A review on regional convection-permitting climate modelling: Demonstrations, prospects, and challenges. *Review of Geophysics*, **53** (2), 323-361. https://doi.org/10.1002/2014RG000475

Pryor S. C., and Coauthors (2009): Wind speed trends over the contiguous United States. *Journal of Geophysical Research – Atmospheres*, **114**, D14105. https://doi.org/10.1029/2008JD011416

Punkka A.-J., & Bister M. (2015): Mesoscale convective systems and their synoptic-scale environment in Finland. *Weather and Forecasting*, **30** (1), 182-196. https://doi.org/10.1175/WAF-D-13-00146.1

R Core Team (2020): R: A language and environment for statistical computing. R Foundation for Statistical Computing, Vienna. http://softlibre.unizar.es/manuales/aplicaciones/r/fullrefman.pdf

Ramon J., Lledó L., Torralba V., Soret A., & Doblas-Reyes F. J. (2019): What global reanalysis best represents near-surface winds? *Quarterly Journal of the Royal Meteorological Society*, **145**, 3236-3251. https://doi.org/10.1002/qj.3616

Rayner D. P. (2007): Wind run changes: The dominant factor affecting pan evaporation trends in Australia. *Journal of Climate*, **20** (14), 3379-3394. https://doi.org/10.1175/JCLI4181.1

Renew Energy policy Network for the 21st century (REN21) (2020): Renewables 2010 Global Status Report. REN21 Secretariat, Paris. https://www.ren21.net/wp-content/uploads/2019/05/gsr_2020_full_report_en.pdf

Rockel B., & Woth K. (2007): Extremes of near-surface wind speed over Europe and their future changes as estimated from an ensemble of RCM simulations. *Climatic Change*, **81**, 267-280. https://doi.org/10.1007/s10584-006-9227-y

Roderick M. L., Rotstayn L. D., Farquhar G. D., & Hobbins M. T. (2007): On the attribution of changing pan evaporation. *Geophysical Research Letters*, **34**, L17403. https://doi.org/10.1029/2007GL031166

Rotach M. W., Gohm A., Lang M. N., Leukauf D., Stiperski I., & Wegner J. S. (2016): On the vertical exchange of heat, mass, and momentum over complex, mountainous terrain. *Frontiers in Earth Science*, **3**, 76. https://doi.org/10.3389/feart.2015.00076

Saha S., and Coatuhors (2010): The NCEP climate forecast system reanalysis. . *Bulletin of the American Meteorological Society*, **91** (8), 1015-1058. https://doi.org/10.1175/2010BAMS3001.1

Serafin S., and Coauthors (2018): Exchange processes in the Atmospheric Boundary Layer over mountainous terrain. *Atmosphere*, **9**, 102. https://doi.org/10.3390/atmos9030102

Sheridan P. (2011): Review of techniques and research for gust forecasting and parametrisation. Forecasting Research Technical Report 570.

Shi P., Zhang G., Kong F., Chen D., Azorin-Molina C., & Guijarro J. A. (2019): Variability of winter haze over the Beijing-tianjin-Habei region tied to wind speed in the lower troposphere and particulate sources. *Atmospheric Research*, **215**, 1-11. https://doi.org/10.1016/j.atmosres.2018.08.013

Slivinski L. C., and Coauthors (2019): Towards a more reliable historical reanalysis: Improvements for version 3 of the Twentieth Century Reanalysis system. *Quarterly Journal of the Royal Meteorological Society*, **145** (724), 2876-2908. https://doi.org/10.1002/qj.3598

Stepanek P. (2004): AnClim:Software for time series analysis and homogenization. http://www.climahom.eu/software-solution/anclim

Strandberg G., and Coauthors (2014): CORDEX scenarios for Europe from the Rossby Centre regional climate model RCA4. SMHI Report Meteorology and Climatology 116. https://www.smhi.se/polopoly_fs/1.90275!/Menu/general/extGroup/attachmentColHold/mainCol1/file/RMK_116.pdf

Suomi I., Vihma T., Gryning S.-E-, & Fortelius C. (2013): Wind-gust parametrizations at heights relevant for wind energy: a study based on mast observations. *Quarterly Journal of the Royal Meteorological Society*, **139** (674), 1298-1310. https://doi.org/10.1002/qj.2039

Suomi I., Gryning S.-E., Floors R., Vihma T., & Fortelius C. (2014): On the vertical structure of wind gusts. *Quarterly Journal of the Royal Meteorological Society*, **141** (690), 1658-1670. https://doi.org/10.1002/qj.2468

Swart N. C., and Coauthors (2019): The Canadian Earth System Model version 5 (CanESM5.03). *Geoscientific Model Development*, **12**, 4823-4873. https://doi.org/10.5194/gmd-12-4823-2019

Swedish Commission on Climate and Vulnerability, 2007. Sweden facing climate change – threats and opportunities. Final report from the Swedish Commission on Climate and Vulnerability. SGO Reports 60. https://www.government.se/49b75f/contentassets/5f22ceb87f0d433898c918c2260e51aa/sweden-facing-climate-change-sou-200760

Taylor K. E., Stouffer E. J., & Meehl G. A. (2012): An overview of CMIP5 and the experiment design. *Bulletin of the American Meteorological Society*, **93** (4), 485-498. https://doi.org/10.1175/BAMS-D-11-00094.1

Thorne P. W., & Vose R. S. (2010): Reanalyses suitable for characterizing long-term trends. *Bulletin of the American Meteorological Society*, **91** (3), 353-362. https://doi.org/10.1175/2009BAMS2858.1

Tokinaga H., & Xie S.-P. (2011): Wave- and anemometer-based sea surface wind (WASWind) for climate change analysis. *Journal of Climate*, **24** (1), 267-285. https://doi.org/10.1175/2010JCLI3789.1

Torralba V., Doblas-Reves F. J., & Conzalez-Reviriego N. (2017): Uncertainty in recent near-surface wind speed trends: a global reanalysis intercomaprison. *Environamental Research Letters*, **12** (11), 114019. https://doi.oeg/10.1088/1748-9326/aa8a58

UK Met Office (1993): Forecasters' Reference Book. Crown, Bracknell, pp. 191

Ulbrich U., Leckebush G. C., & Donat M. G. (2013): Windstorms, the most costly natural hazard in Europe. In *Natural disasters and adaptation to climate change*. Cambridge University Press, Cambridge, pp. 109-120

van Meijgaard E., van Ulft L. H., Lenderink G., de Roode S. R., Wipfler L., Boers R., & Timmermans R. M. A. (2012): Refinement and application of a regional atmospheric model for climate scenario calculations of Western Europe. KVR report 054/12. https://library.wur.nl/WebQuery/wurpubs/fulltext/312258

Vautard R., Cattiaux J., Yiou P., Thépaut J.-N., & Ciais P. (2010): Northern Hemisphere atmospheric stilling partly attributed to an increase in surface roughness. *Nature Geoscience*, **3**, 756-761. https://doi.org/10.1038/NGEO979

Vautard R., and Coauthors (2019): Human influence on European winter wind storms such as those of January 2018. *Earth System Dynamics*, **10** (2), 271-286. https://doi.org/10.5194/esd-10-271-2019

Visbeck M. H., Hurrell J. W., Polvani L., & Cullen H. M. (2001): The North Atlantic Oscillation: Past, present, and future. *Proceeding of the national Academy of Sciences of the United States of America*, **98** (23), 12876-12877. https://doi.org/10.1073/pnas.231391598

Voldoire A., and Coauthors (2019): Evaluation of CMIP6 DECK experiments with CNRM-CM6-1. *Journal of Advances in Modeling Earth Systems*, **11** (7), 2177-2213. https://doi.org/10.1029/2019MS001683

Wallace J. M., & Gutzler, D. S. (1981): Teleconnections in the geopotential height field during the northern hemisphere winter. *Monthly Weather Review*, **109** (4), 784-812. https://doi.org/10.1175/1520-0493(1981)109<0784:TITGHF>2.0.CO;2

Wallemacq P., Below R, & McLean D. (2018): Economic losses, poverty and disasters: 1998-2017. Centre for Research on the Epidemiology of Disasters (CRED) https://www.unisdr.org/files61119_credeconomiclosses.pdf

Wan H., Xiolan L., Wang L., & Swail V. R. (2010): Homogenization and trend analysis of Canadian near-surface wind speeds. *Journal of Climate*, **23** (5), 1209-1225. https://doi.org/10.1175/2009JCLI3200.1

Weggel J. R. (1999): Maximum daily wind gusts related to mean daily wind speed. *Journal of Structural Engineering*, **125**, 465-468. https://doi.org/10.1061/(ASCE)0733-9445(1999)125:4(465)

Wehrli K., Guillod B. P., Hauser M., Leclair M., & Seneviratne S. I. (2018): Assessing the dynamic versus thermodynamic origin of climate model biases. *Journal of Geophysical Research – Atmospheres*, **45** (16), 8471-8479. https://doi.org/10.1029/2018GL079220

Wern L., & Bärring L. (2009): Sveriges vindklimat 1901-2008: Analys av förändring I geostrofisk vind. Meteorologi 138. http://www.smhi.se/polopoly_fs/1.7843!/meteorologi_138.pdf

Wever N. (2012): Quantifying trends in surface roughness and the effect on surface wind speed observations. *Journal of Geophysical Research – Atmospheres*, **117**, D11104. https://doi.org/10.1029/2011JD017118

Wohland J., Omrani N.-E., Witthaut D., & Keenlyside N. S. (2019): Inconsistent wind speed trends in current twentieth century reanalyses. *Journal of Geophysical Research – Atmospheres*, **124** (4), 1931-1940. https://doi.org/10.1029/2018JD030083

World Meteorological Organization (WMO) (1987): The measurement of gustiness at routine wind stations – A review. IOM Report 31. https://library.wmo.int/index.php?lvl=notice_display&id=15514#.XyFHOVCxX_Q

World Meteorological Organization (WMO) (2014): Guide to meteorological instruments and methods of observations. WMO Publication 8. https://www.weather.gov/media/epz/mesonet/CWOP-WMO8.pdf

Wu J., Zha J., Zhao D., & Yang Q. (2018): Changes in terrestrial near-surface wind speed and their possible causes: an overview. *Climate Dynamics*, **51**, 2039-2078. https://doi.org/10.1007/s00382-017-3997-y

Young I. R., & Ribal A. (2019): Multiplatform evaluation of global trends in wind speed and wave height. *Science*, **364** (6440), 548-552. https://doi.org/10.1126/science.aav9527

Yu J., Zhou T., Jiang Z., & Zou L. (2019): Evaluation of near-surface wind speed changes during 1979 to 2011 over China based on five reanalysis datasets. *Atmosphere*, **10** (12), 804. https://doi.org/10.3390/atmos10120804

Yupeng L., Yaning C., & Zhi L. (2019): Effects of land use and cover change on surface wind speed in China. *Journal of Arid Land*, **11**, 345-356. https://doi.org/10.1007/s40333-019-0095-5

Zeng Z., and Coauthors (2018): Global terrestrail stilling: does Earth's greening play a role? *Environmental Research Letters*, **13**, 124013. https://doi.org/10.1088/1748-9326/aaea84

Zeng Z., and Coauthors (2019): A reversal in global terrestrial stilling and its implications for wind energy production. *Nature Climate Change*, **9**, 979-985. https://doi.org/10.1038/s41558-019-0622-6

Zhang Z., Wang K., Chen D., Li J., & Dickinson R. (2019): Increase in surface friction dominates the observed surface wind speed decline during 1973-2014 in the Northern Hemisphere lands. *Journal of Climate*, **32** (21), 7421-7435. https://doi.org/10.1175/JCLI-D-18-0691.1

Zhang G., and Coauthors (2020): Variability of daily maximum wind speed across China, 1975-2016: An examination of likely causes. *Journal of Climate*, **33** (7), 2793-2816. https://doi.org/10.1175/JCLI-D-19-0603.1

Zhang Z., & Wang K. (2020): Stilling and recovery of the surface wind speed based on observations, reanalysis, and geostrophic wind theory over China from 1960 to 2017. *Journal of Climate*, **33** (10), 3989-4008. https://doi.org/10.1175/JCLI-D-19-0281.1

Publications I-VI

I. Safaei Pirooz A. A., Flay R. G. J., **Minola L.**, Azorin-Molina C., & Chen D. (2020): *Effects of sensor response and moving average filter duration on maximum wind gust measurements.* Journal of Wind Engineering & Industrial Aerodynamics, 206, 104354

II. Deng K., Azorin-Molina C., **Minola L.**, Zhang G., & Chen D. (2020): *Global near-surface wind speed changes over the last decades revealed by global reanalyses and CMIP6 model simulations*. Revision submitted to Journal of Climate

III. **Minola L.**, Azorin-Molina C., Guijarro J. A., Zhang G., Son S.-W., & Chen D. (2020): *Climatology of near-surface daily peak wind gusts across Scandinavia: observations and model simulations*. Submitted to Journal of Geophysical Research - Atmospheres

IV. **Minola L.**, Zhang F., Azorin-Molina C., Safaei Pirooz A. A., Flay R. G. J., Hersbach H., & Chen D. (2020): *Near-surface mean and gust wind speeds in ERA5 across Sweden: towards an improved gust parametrization*. Climate Dynamics, 55, 887-907

V. **Minola L.**, Azorin-Molina C., & Chen D. (2016): *Homogenization and assessment of observed near-surface wind speed trends across Sweden, 1956-2013.* Journal of Climate, 29, 7397-7415

VI. **Minola L.**, Reese H., Lai H.-W., Azorin-Molina C., Guijarro J. A., Son S.-W., & Chen, D. (2020). *Wind stilling-reversal across Sweden: The impact of land-use and large-scale atmospheric circulation changes*. Submitted to International Journal of Climatology